ICP/EXT-04-00253

Colloidal Plutonium at the OU 7-13/14 Subsurface Disposal Area: Estimate of Inventory and Transport Properties

Thomas A. Batcheller
George D. Redden

Idaho Completion Project

Bechtel BWXT Idaho, LLC

May 2004

ICP/EXT-04-00253
Project No. 23378

Colloidal Plutonium at the OU 7-13/14 Subsurface Disposal Area: Estimate of Inventory and Transport Properties

Thomas A. Batcheller
George D. Redden

May 2004

Idaho Completion Project
Idaho Falls, Idaho 83415

Prepared for the
U.S. Department of Energy
Assistant Secretary for Environmental Management
Under DOE Idaho Operations Office
Contract DE-AC07-99ID13727

ABSTRACT

This document reports an estimate of the fraction of plutonium buried at the Subsurface Disposal Area likely to be in the form of particulate PuO_2 and provides an estimate of the size distribution of the particulates to quantify the amount of colloidal plutonium. As a colloid, particulate PuO_2 could be transported more rapidly than soluble species of plutonium and therefore must be considered in evaluating the potential for groundwater contamination by plutonium.

An estimated 3.7% (41.9 kg) of plutonium from Rocky Flats Plant shipments are in a particle-size range of less than 1 μm and could migrate as colloids. Evaluation of the statistical uncertainties provides a 95% upper confidence-limit estimate of 4.9% (55.5 kg) of colloid-size plutonium. This report summarizes a review of current literature on colloidal transport to provide an analysis of the potential for colloidal PuO_2 to be mobilized by infiltrating water under the geochemical and hydrological conditions expected at the Subsurface Disposal Area. The Subsurface Disposal Area is a radioactive waste landfill at the Radioactive Waste Management Complex within the Idaho National Engineering and Environmental Laboratory.

Parameters are recommended for use in modeling PuO_2 colloidal transport at the Subsurface Disposal Area to provide a method to calculate plutonium exposure concentrations in groundwater. For release from buried waste and migration through surficial sediments and all basalt units, a K_d of 0 mL/g is recommended for colloidal plutonium. This reflects the potential mobility of colloids in high flow-velocity, low ionic-strength regimes that could exist during flooding or snowmelt conditions in the Subsurface Disposal Area. High flow velocities would persist as water moved down through fractured basalt. Once percolating water encounters a sedimentary interbed, the flow velocity will decrease and the ionic strength will increase. Under these hydrochemical conditions, colloids will be filtered out of percolation and will sorb to interbeds. Because no mechanism creates high flow velocities in interbeds, this colloidal plutonium, once sorbed, will not be remobilized in colloidal form. The mechanism to remobilize this plutonium will be dissolution and transport in the dissolved phase. For release and subsequent transport of this plutonium from interbeds, the dissolved-phase plutonium K_d of 2,500 mL/g should be used.

This report supports future development of the Waste Area Group 7 remedial investigation and feasibility study for Operable Unit 7-13/14. Data developed in this report provide a basis for supporting future risk management decisions for Waste Area Group 7 under the Comprehensive Environmental Response, Compensation and Liability Act as outlined in the *Federal Facility Agreement and Consent Order for the Idaho National Engineering Laboratory*.

CONTENTS

FIGURES

TABLES

ACRONYMS

BARF	batch ash Rocky Flats virgin (i.e., in the condition received) incinerator ash
BARF RC	batch ash Rocky Flats rotary-calcined incinerator ash
cum.wt%<	cumulative weight percent less than
DLVO	Derjaguin, Landau, Verwey, and Overbeek
HEPA	high-efficiency particulate air
INEEL	Idaho National Engineering and Environmental Laboratory
OU	operable unit
PSD	particle size distribution
RFP	Rocky Flats Plant
RI/FS	remedial investigation and feasibility study
R-R	Rosin-Rammler
RWMC	Radioactive Waste Management Complex
SDA	Subsurface Disposal Area
WAG	waste area group
Z&R	Zodtner and Rogers

Colloidal Plutonium at the OU 7-13/14 Subsurface Disposal Area: Estimate of Inventory and Transport Properties

1. INTRODUCTION

Plutonium is one of the radioactive elements buried in the Subsurface Disposal Area (SDA), which is a radioactive waste landfill within the Radioactive Waste Management Complex (RWMC) at the Idaho National Engineering and Environmental Laboratory (INEEL). Radioactive waste from the Rocky Flats Plant (RFP)[a] was buried at the SDA in unlined pits and trenches from 1954 to 1970 (Holdren et al. 2002). The location of the RWMC in relation to other major facilities at the INEEL is shown in Figure 1.

Field observations of plutonium migration in subsurface environments and results of laboratory column experiments indicate that plutonium may migrate in different forms. While most plutonium shows little mobility, a small fraction of plutonium was observed in laboratory column experiments to move with little retardation (Glover, Miner, and Polzer 1976; Fjeld, Coates, and Elzerman 2000). This mobile fraction has been attributed to colloidal transport. Colloidal transport has been identified as a possible explanation for accelerated subsurface transport of plutonium at the Nevada Test Site (Kersting et al. 1999) and at Los Alamos National Laboratory (Nyhan et al. 1985; Penrose et al. 1990). To adequately assess the mobility of plutonium at the SDA, the potential impact of colloidal transport of plutonium must be analyzed. This report develops information needed for such an assessment.

Knowledge of the amount, form, and potential transport of plutonium buried at the SDA is required to estimate potential risk from ingestion of contaminated groundwater to support future remedial action decisions. Because records of waste shipments to the SDA did not include detailed information about physical and chemical forms of individual waste components, and because direct field data are not available, estimates were derived for these quantities using ancillary information and scientifically defensible methods. Of particular concern is the fraction of plutonium in the form of PuO_2 (plutonium oxide) particles and the potential for this fraction to be mobilized by infiltrating water. This report presents an estimate of the fraction of plutonium inventory buried in the SDA in the form of PuO_2 particles. Also presented is an analysis of potential mobility of colloidal PuO_2 in the context of geological and infiltration properties of the SDA, with recommendations for partition parameters (K_d values) that can be used to model colloidal transport. This study was conducted to support risk and contaminant transport models that are part of the remedial investigation and feasibility study (RI/FS) for Waste Area Group (WAG) 7, Operable Unit (OU) 7-13/14.[b]

1.1 Purpose and Scope

The objectives of this study are to estimate the amount of plutonium in colloidal form in the SDA inventory and to identify distribution coefficients (K_ds) to simulate potential mobility of PuO_2 colloids using existing models (i.e., DOSTOMAN and TETRAD, as described in detail in Holdren et al. [2002]).

---

a. The RFP is located 26 km (16 mi) northwest of Denver. In the mid-1990s, it was renamed the Rocky Flats Environmental Technology Site. In the late 1990s, it was again renamed, to its present name, the Rocky Flats Plant Closure Project.

b. The *Federal Facility Agreement and Consent Order for the Idaho National Engineering Laboratory* (DOE-ID 1991) lists 10 WAGs for the INEEL. Each WAG is subdivided into OUs. The RWMC is identified as WAG 7 and originally contained 14 OUs. Operable Unit 7-13 (transuranic pits and trenches RI/FS) and OU 7-14 (WAG 7 comprehensive RI/FS) were ultimately combined into the OU 7-13/14 comprehensive RI/FS for WAG 7.

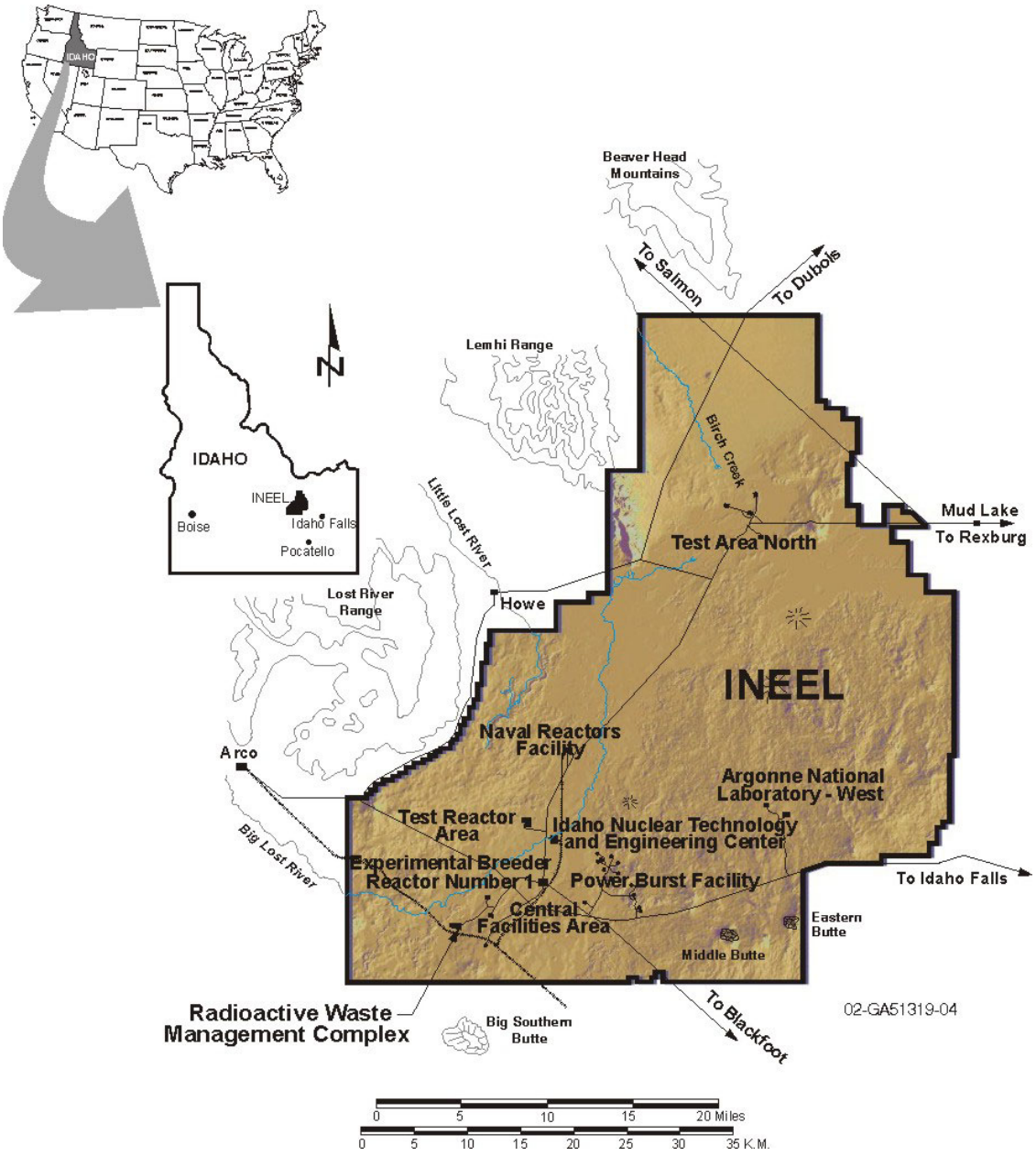

Figure 1. Location of the Radioactive Waste Management Complex and other major facilities at the Idaho National Engineering and Environmental Laboratory.

Because most plutonium in the SDA came from RFP, only RFP plutonium waste streams are addressed in this report.

This information supports development of the WAG 7 RI/FS by providing an estimate of the inventory of plutonium in colloidal form buried in the SDA, an analysis of potential PuO_2 colloidal transport under conditions at the SDA, and a recommendation for parameters to be used in source-release and transport modeling. Data developed in this report provide a basis for supporting future risk-management decisions for WAG 7 under the "Comprehensive Environmental Response, Compensation and Liability Act" (42 USC 9601 et seq., 1980) as outlined in the *Federal Facility Agreement and Consent Order for the Idaho National Engineering Laboratory* (DOE-ID 1991).

1.2 Overview

Plutonium isotopes have been identified as special-case contaminants of concern at the SDA (Holdren and Broomfield 2003). Though plutonium isotopes were not identified as COCs based on risk estimates, Pu-238, Pu-239, and Pu-240 are classified as special-case contaminants of concern to acknowledge uncertainties about plutonium mobility in the environment and to reassure stakeholders that risk management decisions for the SDA will be fully protective. Plutonium colloids (e.g., PuO_2 colloids) are forms of plutonium that could be transported rapidly under certain conditions, unlike soluble plutonium species that strongly adsorb to mineral surfaces under neutral or slightly alkaline field conditions (Flury and Harsh 2003).

An estimate of the fraction of buried plutonium likely to be in a colloidal form and parameter values that should be used in modeling transport of colloids from the waste are required for the OU 7-13/14 RI/FS.

1.3 Site Background

The INEEL, originally established in 1949 as the National Reactor Testing Station, is a U.S. Department of Energy-managed reservation that historically has been devoted to energy research and related activities. The INEEL is located in southeastern Idaho and occupies 2,305 km^2 (890 mi^2) in the northeastern region of the Snake River Plain. Regionally, the INEEL is nearest to the cities of Idaho Falls and Pocatello and to U.S. Interstate Highways I-15 and I-86. The INEEL Site extends nearly 63 km (39 mi) from north to south, is about 58 km (36 mi) wide in its broadest southern portion, and occupies parts of five southeast Idaho counties.

The RWMC, located in the southwestern quadrant of the INEEL, encompasses a total of 72 ha (177 acres) and is divided into three separate areas by function: the SDA, the Transuranic Storage Area, and the administration and operations area. The original landfill, established in 1952, covered 5.2 ha (13 acres) and was used for shallow land disposal of solid radioactive waste. In 1958, the landfill was expanded to 35.6 ha (88 acres). Relocating the security fence in 1988 to outside the dike surrounding the landfill established the current size of the SDA as 39 ha (97 acres). The Transuranic Storage Area was added to the RWMC in 1970. Located adjacent to the east side of the SDA, the Transuranic Storage Area encompasses 23 ha (58 acres) and is used to store, prepare, and ship retrievable transuranic waste to the Waste Isolation Pilot Plant. The 9-ha (22-acre) administration and operations area at the RWMC includes administrative offices, maintenance buildings, equipment storage, and miscellaneous support facilities. Figure 2 contains a map of the RWMC showing the location of the SDA.

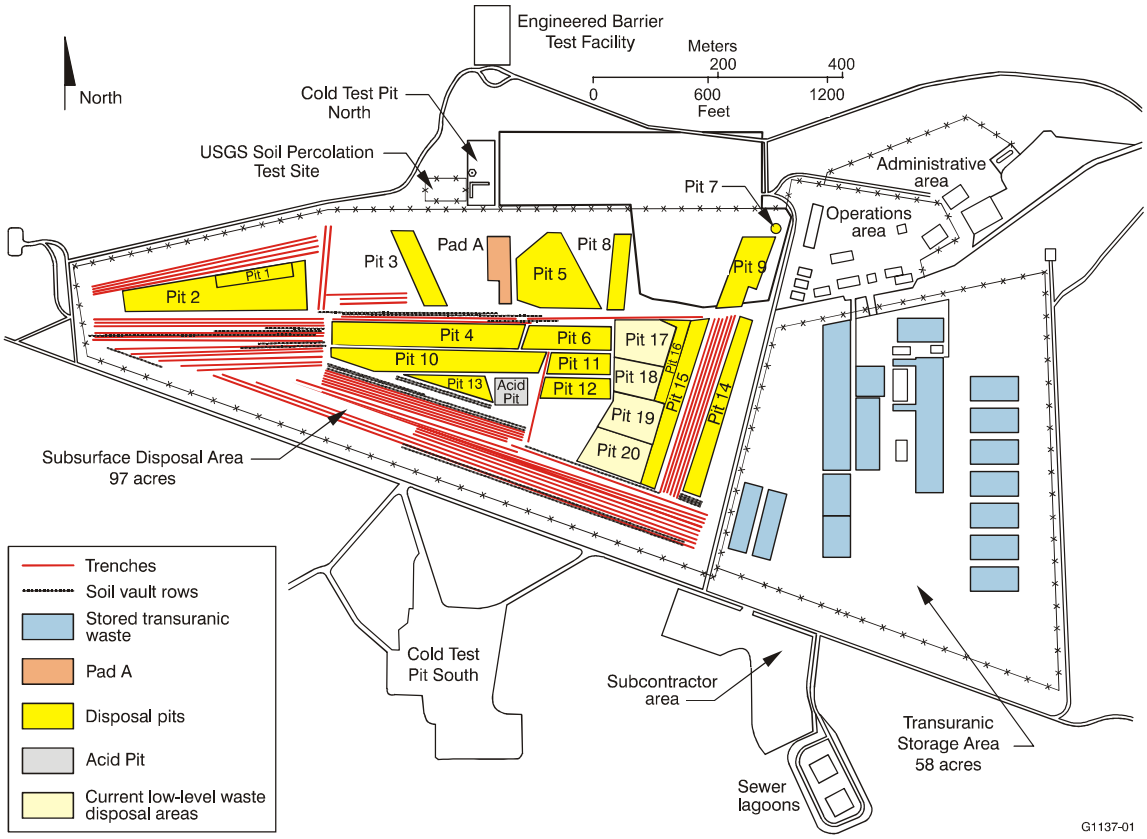

Figure 2. Map of the Radioactive Waste Management Complex showing the location of the Subsurface Disposal Area.

The Snake River Plain Aquifer underlies the RWMC at an approximate depth of 177 m (580 ft) and flows generally northeast to southwest. The aquifer is bounded on the north and south by the edge of the Snake River Plain, on the west by surface discharge into the Snake River near Twin Falls, Idaho, and on the northeast by the Yellowstone basin.

The subsurface below a shallow (approximately 10 m [32 ft]) soil horizon is characterized by alternating layers of fractured basalt and sedimentary deposits called interbeds. The interbeds tend to retard infiltration to the aquifer (McElroy and Hubbell 2004) and are important in determining the rate of transport of contaminants toward the aquifer. Surficial sediments resulting from fluvial, lacustrine, and aeolian deposition are similar to the sedimentary interbeds, though surface sediments are less mature and little stratigraphic layering remains in the soil used to bury waste.

The Snake River Plain is an arid environment with an average annual precipitation of 23 cm/year (9 in./year). Infiltration of water occurs episodically from rain, flood, and snowmelt. The soil horizon at the SDA is unsaturated most of the year and underlying formations are characterized as a vadose zone. This environment constrains what basic processes, laboratory studies, or field data should be considered in evaluating PuO_2 colloid transport.

1.4 Rocky Flats Plant Plutonium Waste Forms Buried in the Subsurface Disposal Area

Most plutonium buried in the SDA originated at RFP. The total estimated plutonium inventory at the SDA is about 1,100 kg. Because the amount of Pu-238 from RFP waste (i.e., 1 kg) is negligible (less than 0.1% of the total plutonium buried in the SDA), Pu-238 is not included in this analysis. Non-RFP plutonium[c] equals 55 kg, which is slightly less than 5% of the total plutonium buried in the SDA. These non-RFP waste streams were not from processes that tend to produce particles (e.g., pyrochemical and calcining processes at RFP); thus, colloidal plutonium from these waste streams is assumed to be negligible. The estimated mass of plutonium in colloidal particles is, therefore, applied only to waste from RFP that contained Pu-239 and Pu-240.

Three general forms of plutonium waste produced at RFP and sent to the SDA are listed below:

- Soluble plutonium complexes from aqueous-phase dissolution processes
- Particulate PuO_2 material produced in the calcination operation and, to a lesser extent, plutonium-bearing particulate material produced in incineration and pyrochemical operations
- Plutonium metal lodged in foundry molds.

Baldwin and Navratil (1983) provide a general overview of the RFP plutonium-recovery processes, and Figure 3-2 from the *Acceptable Knowledge Document for INEL Stored Transuranic Waste—Rocky Flats Plant Waste* (INEEL 2003) augments the process flowsheet presented by Baldwin and Navratil (1983). Wick (1984) and Benedict, Pigford, and Levi (1981) also were reviewed for further RFP information. The following paragraphs provide further descriptions and details of soluble and plutonium-particulate forms and waste-generation mechanisms relative to the process operations described above.

Most plutonium entering the RFP for processing went through aqueous dissolution, separation, and calcining. Solubilized plutonium complexes were adsorbed on ion-exchange resins. Unadsorbed americium associated with plutonium was routed to a separate recovery operation. Adsorbed plutonium was eluted and routed to a peroxide-precipitation operation where solid plutonium oxyhydroxides were formed. Plutonium-contaminated resin-bed packing materials and other equipment containing residual solubilized plutonium were transferred to the SDA for disposal.

The calcining operation converted plutonium peroxide precipitate to PuO_2. Most of the particulate PuO_2 was produced in the calcination phase. Most PuO_2 formed during calcining could be dissolved using conventional methods, though some PuO_2 was refractory (i.e., resistant to treatment, even at high temperatures) and not readily dissolved. Pyrochemical processes (primarily electrorefining) and, to a lesser extent, metal-processing operations, generated smaller amounts of plutonium-particulate material. Slag from the electrorefining metal-button wash and from the calcium-reduction operation was contaminated with plutonium. These slag materials, with any plutonium-bearing particulate material recovered from calcination, incineration, or metal-processing (casting or metal working) operations, were recycled back to the aqueous-leaching and dissolution process.

Most plutonium-particulate material recycled back to the leaching and dissolution process was typically dissolved with a more aggressive acid dissolvent (i.e., HNO_3-HF). Remaining refractory PuO_2 was in the form of small particles (less than 30 μm) that could be carried through the aqueous processing

c. Non-RFP plutonium is identified as coming from an off-INEEL source other than RFP, from an INEEL waste stream, or from miscellaneous minor streams (see Table 5-3 in Holdren et al. [2002]).

train, through the plutonium-peroxide cake stream, and would exit in the peroxide-precipitation overflow. Most particulate material from the leaching and dissolution process was filtered and diverted back for another cycle of leaching and dissolution. Plutonium oxide that accumulated on filters was periodically diverted for waste treatment. Plutonium oxide particles from the filtration operation and precipitation overflow were included in sludge, which was processed in waste treatment operations for disposal. Process knowledge implies most particulate PuO_2 in waste material was the refractory form (INEEL 2003).

Waste stream code numbers, descriptions, and curies of all plutonium-bearing waste streams buried in the SDA are provided in Table 5-3 of the *Ancillary Basis for Risk Analysis of the Subsurface Disposal Area* (Holdren et al. 2002).

1.5 Document Organization

The remaining sections in this report are summarized below:

- Section 2 provides an estimate of the colloidal plutonium buried in the SDA and describes methodology used to establish the estimate
- Section 3 describes the approach used to estimate mobility of colloidal PuO_2 in the SDA environment and suggests appropriate risk-assessment parameters for modeling colloidal plutonium transport
- Section 4 summarizes the report and presents recommendations for modeling
- Section 5 lists references cited in this report.

2. ESTIMATE OF COLLOIDAL PLUTONIUM INVENTORY

Because of uncertainties in the SDA waste inventory (type and quantity), and because direct field data are absent, an inferential analysis is applied to estimate an inventory of particulate plutonium in the SDA. The strategy used to estimate the inventory of plutonium colloidal particulates in waste buried in the SDA is described in the sections listed below. These sections address each step in the analysis.

- Section 2.2—Establish a single equation for particle size distribution (PSD) that is valid for estimating the weight percent of RFP plutonium-particulate material as a function of particle size. A single, generalized distribution for all waste streams is generated rather than a set of individual distributions for each waste stream.

- Section 2.3—Estimate the fraction of each waste stream inventory that would comprise plutonium-particulate material, based on the generating process of the waste stream.

- Section 2.4—Estimate the particle size range of each waste stream identified in Section 2.3, based on process characteristics and factors including filter performance, equipment-decontamination techniques. The maximum particle size (referred to as the upper particle-break size) is particularly important because it is used to calculate the fraction of colloidal material.

- Section 2.5—Calculate the percent-particulate material in the transportable range by inserting the maximum particle break size determined in Section 2.4 into the generalized equation established in Section 2.2.

- Section 2.6—Calculate the amount of particulate material that would be in the transportable range.

- Section 2.7—Determine the uncertainty in the estimate and provide an upper-bound estimate of transportable plutonium.

2.1 Assumptions

A series of engineering estimates were developed because of the absence of direct measurements of colloidal-size plutonium in waste streams sent to the SDA. Each estimate involves assumptions that affect the final estimate. This section summarizes those assumptions and describes the basis for considering the assumptions to be valid. Additional details for each assumption are included in subsequent sections of this report.

- Data on PSDs are representative of RFP processes that generated waste and can be used to estimate RFP PSDs. Some PSD data were gathered from information about RFP waste generated by processes of interest for this report. Other data were gathered on particulate-plutonium emissions from high-temperature processes. These data sources are closely linked to the types and temperatures of processes of interest.

- Composition of plutonium particles is independent of particle size. Data from Behrens et al. (1995) show that the cumulative weight percent of plutonium in RFP incinerator ash has the same distribution as the ash.

- Particle size distributions do not depend on particle composition. Two types of material included in this analysis have different compositions and particle densities. Some materials are PuO_2 and others are ash (silicates) containing plutonium. Cumulative weight percent was calculated separately for

the PuO_2 and the ash so that each cumulative curve contains only data with similar composition and density. This normalized each data set to remove differences in density and composition of the particles.

- Colloidal-size particles are smaller than the size distribution measured in available data sets. To extrapolate to smaller sizes, an equation that is well established and documented in literature is used to describe the PSD. Because this curve fits the size distribution of many different materials from many different sources, confidence is high that it can be used to extrapolate to the colloidal-size range.

- Process studies conducted at RFP indicate that plutonium that was insoluble in concentrated nitric acid was extremely resistant to recycling (Baldwin and Navratil 1983). These residuals would have been retained in ash and sludge processed as waste from RFP operations. These refractory particles would retain their original size distribution in buried waste at the SDA.

2.2 Develop Equation for Particle Size Distribution

Because no data are available for actual PSD in the various SDA waste types, an independent method to estimate PSD of PuO_2 in the SDA is used to estimate weight percent of plutonium-particulate material in a given waste stream as a function of particle size. A literature search produced several sets of plutonium-material PSD data, the applicability and significance of which are discussed in the following subsections.

2.2.1 Data Sets for Developing an Equation for Particle Size Distribution

Data on sieving and particle-size fractionation of actual RFP incinerator ash particulate material (Behrens et al. 1995) include batch ash Rocky Flats virgin incinerator ash (BARF) and batch ash Rocky Flats rotary-calcined incinerator ash (BARF RC) (see Table 1). Although limited, these sample weight-percent data are valuable because (1) these RFP ash material samples reasonably represent particulate material buried in the SDA and (2) samples cover the entire size range of interest for this inventory estimate because no material was removed from the upper or lower ends of the PSD (e.g., fines)

Table 1. Cumulative weight-percent data on Rocky Flats sieved virgin and rotary-calcined incinerator ash and Curve D representing PuO_2 derived from burning plutonium metal.

Particle Size (μm)	Cumulative Weight Percent Less Than					
	BARF1	BARF2	BARF3	BARF1RC	BARF2RC	Curve D
0.5	—	—	—	—	—	0.01
1	—	—	—	—	—	0.03
3	—	—	—	—	—	0.1
10	—	—	—	—	—	0.3
88	3.1	12.1	4.9	1.4	3.2	—
175	15.2	55.3	15.8	6	10.3	—
351	38.2	98	34.7	49.2	42.1	—

or any portion of the samples. *Cumulative weight percent less than* (expressed as cum.wt%<) distributions were generated from these data (see Figure 3). Five data sets from Behrens et al. (1995) (i.e., BARF1, BARF2, BARF3, and BARF1RC, and BARF2RC) were used in this analysis.

Additional data that closely represent particulate material buried in the SDA are available from a study that used cascade-impactor PSD analyzer technology to obtain data in the 1–100-µm range of PuO_2 particulate materials (Stewart 1963). Stewart (1963) investigated PSD of PuO_2 formed upon oxidation of plutonium metal by corrosion or combustion to evaluate the worker-exposure risk from airborne plutonium in the laboratory. The PSD of the PuO_2 oxide after oxidation depended on the form of the initial plutonium, the temperature of the reaction, and the rate of the reaction, with temperature being the most important factor. Data from the individual experiments were combined into four cumulative weight-percent curves based on reaction temperature (Stewart 1963, Figure 12). Because incineration and calcining operations at RFP were above 900˚C (Beheren et al. 1995), Curve D is the most applicable curve presented by Stewart (1963). Data from Curve D of Stewart (1963) are included in the analysis. Data from other curves presented by Stewart are for lower temperature conditions, or are for air emissions and are less representative of RFP waste streams.

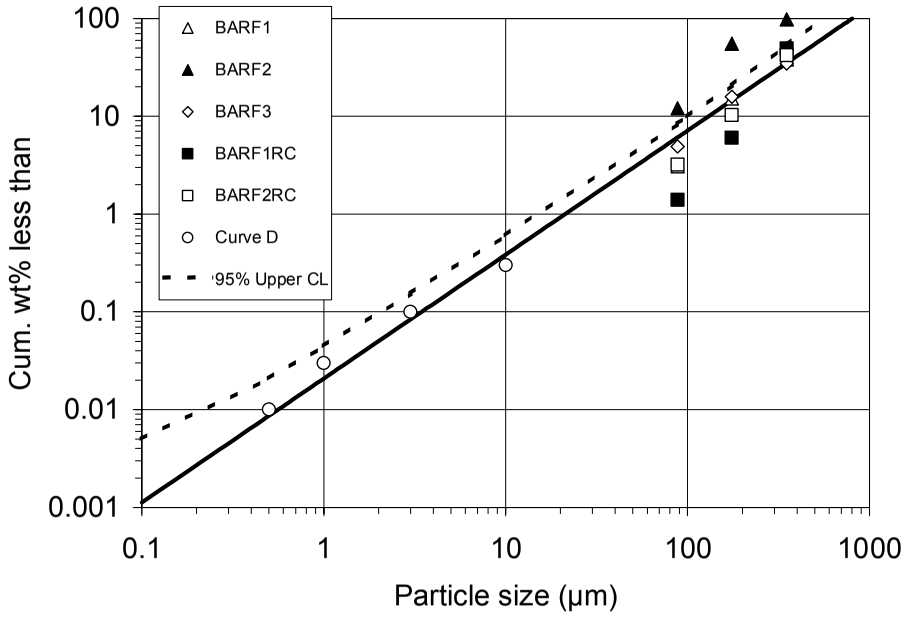

Figure 3. Comparison of data from sieved batch ash Rocky Flats virgin incinerator ash with data from combustion of plutonium above the ignition temperature (Curve D), shown with a least-squares-fit to the data along with the 95% upper-confidence limit for the fit.

2.2.2 Equation for Particle Size Distribution

A common equation used to represent cumulative distributions as a straight line is the Rosin-Rammler (R-R) model fit (Perry 1984; Allen 1990). This model is used here to obtain an expression adequate for estimating cumulative weight percent of plutonium-particulate material as a function of particle size. All data sets presented in the previous section are potentially relevant to PSD of waste buried in the SDA. All of the data were used to develop a single curve using a least-squares-regression analysis.

Parameters for the R-R fit of these data are provided in Table 2 and graphically illustrated in Figure 3. Equation (1) presents the PSD equation for estimating weight percent of plutonium-particulate material as a function of particle size.

Table 2. Parameters for Rosin-Rammler fit to cumulative plutonium-particle-size data.

	Coefficient	Standard Error	Lower 95% Confidence Limit	Upper 95% Confidence Limit
Intercept	-1.6809	0.1586	-2.0156	-1.3463
Slope	1.2673	0.0784	1.1019	1.4327

$$\log_{10}\left[Cum\,wt\%<\right] = 1.2673 \times \log_{10}\left[d_{particle\,(in\,\mu m)} \right] - 1.6809 \quad . \tag{1}$$

This fit provides a statistically significant reduction in the residual sum of squares. The coefficient of determination of 0.935 indicates that 93.5% of data uncertainty is accounted for by the R-R fit (Charpa and Canale 1988). These results do not reflect the uncertainty of how accurately this fit represents plutonium-particulate material buried in the SDA. That topic is discussed further in Section 2.7.

2.3 Estimate of Particle Fraction in Waste Streams

The following subsections present background information used for estimating the fraction of RFP plutonium waste that would be particulate material.

2.3.1 Waste Stream Data and Information for Estimating the Colloidal Inventory

A general overview of the RFP plutonium-recovery processes is available from Baldwin and Navratil (1983). Figure 3-2, "Pu production, recovery and purification flow diagram," in INEEL (2003) augments the process flowsheet figure presented in the Baldwin and Navratil (1983) paper. Further RFP details were reviewed in Wick (1984).

Plutonium curie data presented in Table 5-3 in the *Ancillary Basis for Risk Analysis* (Holdren et al. 2002) were translated for this report to better align with RFP waste-generation processes based on information from Zodtner and Rogers (1964). Results of the realignment are presented in Table 3. These data also are used in the estimated inventory of colloidal plutonium-particulate material in the SDA. Note that curie amounts have not been changed; curie amounts only have been reallocated to reflect a more accurate picture of their distribution in the waste streams during the periods based on these references.

In 1964, disposal procedures and controls at RFP were changed due to findings and recommendations from Zodtner and Rogers (1964). Therefore, RFP waste was divided into the following two periods:

1. Waste delivered to the SDA from 1954 through 1963.

2. Waste delivered to the SDA from 1964 (when Zodtner and Rogers' recommendations were implemented) through 1970, when burial of plutonium waste in the SDA ended.

Table 3. Adjusted Rocky Flats Plant plutonium curies buried in the Subsurface Disposal Area; 1954–1963 and 1964–1970 periods.

1954–1963	Pu-239		Pu-240		Total Pu-239 and Pu-240	
Description	(Ci)	(kg)	(Ci)	(kg)	(Ci)	(kg)
RFP Bldg 776 ventilation prefilters on pyrochemical (i.e., purification, refining, and production) processes (foundry operations were in RFP Bldg 776 until the 1969 fire).	1.932E+02	3.1	4.294E+01	0.2	2.362E+02	3.3
RFP Bldg 771 ventilation prefilters on aqueous, calcination, and fluorination and reduction (i.e., recovery and refining) processes.	7.354E+03	118.6	1.634E+03	7.2	8.989E+03	125.8
Graphite: old-type graphite molds (p. 11).[a]	1.487E+04	239.8	3.310E+03	14.6	1.818E+04	254.3
RFP Bldg 774 aqueous first-stage water treatment of Series 741 sludge.	2.284E+03	36.8	5.075E+02	2.2	2.791E+03	39.1
Type V RFP Bldg 776 drybox noncombustible waste (e.g., scrap iron, broken glass, and heavy rubber gloves) (p. 10).[a]	1.036E+03	16.7	2.303E+02	1.0	1.267E+03	17.7
RFP Bldg 776 drybox washable waste (all rubber and plastic-type materials) (p. 10).[a]	1.651E+03	26.6	3.669E+02	1.6	2.018E+03	28.2
Type V RFP Bldg 771 drybox noncombustible waste (e.g., scrap iron, broken glass, and heavy rubber gloves) (p. 10).[a]	1.118E+03	18.0	2.485E+02	1.1	1.367E+03	19.1
Totals 1954–1963	2.851E+04	459.6	6.340E+03	27.9	3.485E+04	487.5

Table 3. (continued).

1964–1970	Pu-239		Pu-240		Total Pu-239 and Pu-240	
Description	(Ci)	(kg)	(Ci)	(kg)	(Ci)	(kg)
Type I combustibles: paper, rags, plastic, clothing, cardboard, wood, and poly bottles; most of this is assumed to be from RFP Bldg 771 aqueous-type operations (i.e., operations, waste treatment, and laboratory work).	3.257E+03	52.5	7.286E+02	3.2	3.986E+03	55.7
Type II waste (e.g., glass Raschig rings not lumped into Type V noncombustible waste).	2.935E+03	47.3	6.572E+02	2.9	3.592E+03	50.2
Type III HEPA filters; from RFP Bldg 776 pyrochemical processes, RFP Bldg 771 (calcination), and foundry operations.	4.321E+03	69.7	9.675E+02	4.3	5.289E+03	73.9
Type V noncombustible waste generated outside the drybox-line processes.	7.363E+03	118.7	1.650E+03	7.3	9.013E+03	126.0
Line-generated waste: Type V noncombustible waste generated inside the drybox production-line processes.	9.313E+03	150.1	2.088E+03	9.2	1.140E+04	159.3
Graphite molds from the foundry and production line.	1.842E+03	29.7	4.130E+02	1.8	2.255E+03	31.5
RFP Bldg 774 aqueous first-stage water treatment Series 741 sludge.	5.137E+03	82.8	1.150E+03	5.1	6.286E+03	87.9
RFP Bldg 774 organic Series 743 sludge.	1.579E+02	2.5	3.536E+01	0.2	1.933E+02	2.7
RFP Bldg 774 special setups Series 744 sludge.	1.827E+02	2.9	4.092E+01	0.2	2.236E+02	3.1
RFP Bldg 774 aqueous evaporator-bottoms salt and sludge; Series 745 sludge.	5.821E+00	0.1	3.565E-01	0.0	6.178E+00	0.1
Totals 1964–1970	3.451E+04	556.4	7.730E+03	34.1	4.224E+04	590.5
Totals 1954–1970	6.302E+04	1016.0	1.407E+04	62.0	7.7095E+04	1,078.0

a. Zodtner and Rogers 1964.
HEPA = high-efficiency particulate air RFP = Rocky Flats Plant

2.3.2 Estimate Fraction of Particulate Material

Several RFP processes generated particulate material. These processes were considered in estimating the *fraction* of plutonium in particulate form buried at the SDA. The following paragraphs describe these processes.

2.3.2.1 Building 771 Processes. In RFP Bldg 771, a calcination operation converted the plutonium-peroxide precipitate to PuO_2 (Baldwin and Navratil 1983; Wick 1984 [Section 16-1]). It was assumed that calcination generated most of the RFP indissolvable refractory particulate PuO_2 material (i.e., indissolvable in nitric acid, more dissolvable in HNO_3-HF dissolvent, but still not 100%). Most of the PuO_2 from calcination is fluorinated (to PuF_4) and then reduced to plutonium metal with calcium. Some PuO_2 was not converted to plutonium metal and remained with the reduction slag, and the reduction slag was recycled back to the Bldg 771 dissolution process. Particulate material embedded in Bldg 771 high-efficiency particulate air (HEPA) filters (prefilters) was primarily due to entrainment emissions from the calcination operation and was, therefore, assumed to be refractory particles. Particulate material also was dispersed, settled, and adhered in and on surfaces inside the Bldg 771 drybox (e.g., Type V noncombustible waste: scrap iron, glass, and equipment). A portion of the contaminated material was assumed to be contaminated with refractory particles.

Indissolvable refractory particulate PuO_2 (produced in the calcination and incineration processes) would eventually be shunted from Bldg 771 dissolution processes (i.e., dissolution, leaching, and filtration) to Bldg 774 sludge treatment operations.

During foundry operations, metal was caught in graphite casting molds, especially in the 1954-1963 era (Zodtner and Rogers 1964). This metal was converted to PuO_2 and nearly all of it was dissolvable in dissolution operations. This also was assumed for other production-metal scraps recycled to the dissolution process. However, any burned or incinerated metal would contain some quantity of indissolvable particulate.

2.3.2.2 Building 776 Processes. A pyrochemical refining process was carried out in RFP Bldg 776. It was assumed that particulate material trapped in Bldg 776 HEPA filters (prefilters) was primarily due to entrainment emissions from refining operations (primarily electrorefining [Wick 1984, Section 15-2.2{b}]). These emission amounts were substantially smaller than those for Bldg 771. Similar to Bldg 771, particulate material was dispersed, settled, and adhered in and on surfaces inside the Bldg 776 drybox (i.e., Type V noncombustible waste). It was assumed that a small amount of the indissolvable refractory particulate material was generated in Bldg 776 operations.

Based on these assumptions and the references cited, waste stream *fraction* of particulates was estimated. Assumptions and estimates are shown in Table 4. Effects of the precision of these estimates are discussed in Section 2.7.

2.4 Estimate Range of Particle Sizes

Reference information discussed in Section 2.3 was used to estimate the particle-size range of material originally buried in the SDA. Assumptions and estimates are shown in Table 4. Effects of the precision of these estimates are discussed in Section 2.7. Plutonium that is not particulate is assumed to be molecular-scale soluble species. Particle-range break sizes were estimated using engineering information from *Perry's Chemical Engineers' Handbook* (Perry 1984), the Stanford Research Institute particle characteristics chart (see Figure 4 for an excerpt) from Perry (1984), and from the Geldart powder classification chart (Geldart 1986) presented in Figure 5.

Table 4. Estimated inventory of colloidal plutonium buried in the Subsurface Disposal Area.

1954–1963		Best Estimate				Upper Limit		
Waste Stream	Estimation Bases and Assumptions	Fraction Particulate	Upper Break (µm)	Percent Particulates in Transportable Range (%)	Inventory in Transportable Range (kg)	Fraction Particulate	Percent Particulates in Transportable Range (%)	Inventory in Transportable Range (kg)
Series 776 Drybox prefilters	All plutonium curies due to Bldg 776 pyrochemical process emissions, and all is particulate. Most of this material is probably <u>not</u> the difficult-to-dissolve refractory form. Estimated a 45-µm upper break size using the "metallurgical dusts and fumes" line in the particulate characteristics chart in Figure 20-102 in *Perry's Chemical Engineers' Handbook*;[a] assumed same terminal velocity and adjusted the 100-µm upper break size with SQRT($\rho_{typical\ metal}/\rho_{Pu}$) = SQRT(50/244).	1.00	45	0.80	0.027	1.00	1.24	0.41
Series 771 Drybox prefilters	All plutonium curies due primarily to Bldg 771 calcination process emissions and nonfluorinated or nonreduced plutonium in the reduction slag; assuming most is particulate, but small amount of soluble form from aqueous operations; some of this material <u>is</u> probably the difficult-to-dissolve refractory type. Same as for Bldg 776, the 45-µm upper break size is used.	0.90	45	0.80	0.909	1.00	1.24	1.559
Graphite	Plutonium metal in "old type" graphite molds; majority of the PuO_2 formed from this material is <u>not</u> the difficult-to-dissolve refractory type. Used 100%-intercept of 735 µm from final R-R fit as upper break size.	1.00	735	0.02	0.059	1.00	0.03	0.079
Series 741 sludge	All sludge plutonium curies <u>are</u> composed of the difficult-to-dissolve refractory PuO_2 form generated primarily in the Bldg 771 calcination process, and any process where plutonium was "burned." This sludge is primarily from underflow from the Bldg 771 aqueous dissolution, leaching, and filtration processes. Based on *Perry's Chemical Engineers' Handbook*[a] Section 19, "Filtration"; assumed a 3-µm upper break size.	1.00	3.0	24.85	9.704	1.00	29.04	11.339
Series 776 Type V Noncombustibles inside drybox	All plutonium curies due to Bldg 776 pyrochemical processes. Particulate material was dispersed, settled, and adhered in and on surfaces inside drybox. Most of this material is probably <u>not</u> the difficult-to-dissolve refractory type. Estimated 0.90 fraction particulate from words in the Z&R report[b]—". . .scrap iron, broken glass. . . generated inside the drybox and processing lines"—noncombustible waste—assuming some amount of soluble form on surfaces. Estimated a 300-µm upper break size using ". . .superficial cleaning. . ." words in Z&R report;[b] and, using the Geldart powder classification diagram (Geldart 1986[c] [see Figure 9])—assuming "Group D" particles (with density ~10) were removed with the superficial cleaning.	0.90	300	0.07	0.012	1.00	0.10	0.18

Table 4. (continued).

1954–1963		Best Estimate				Upper Limit		
Waste Stream	Estimation Bases and Assumptions	Fraction Particulate	Upper Break (µm)	Percent Particulates in Transportable Range (%)	Inventory in Transportable Range (kg)	Fraction Particulate	Percent Particulates in Transportable Range (%)	Inventory in Transportable Range (kg)
Washables inside drybox	All plutonium curies due to Bldg 776 pyrochemical processes. Again, most of this material is probably not the difficult-to-dissolve refractory type. Estimated 0.90 fraction particulate from words in the Z&R report[b]—". . .rubber and plastic type materials"—assuming some amount of soluble plutonium on surfaces. Assumed a 20-µm upper break size using the Geldart[c] powder classification diagram—assuming only cohesive particles left on surfaces.	0.90	20	2.24	0.570	1.00	3.29	0.930
Series 771 Type V Combustibles inside drybox	Same basis as used for Bldg 776 noncombustible waste. Particulate material was dispersed, settled, and adhered in and on surfaces inside drybox. Again, some of this material is probably the difficult-to-dissolve refractory type. Assumed a greater amount of soluble plutonium form on surfaces.	0.75	300	0.07	0.010	1.00	0.10	0.020
Total 1954–1963 SDA plutonium in transportable range (kg) =					11.29			13.99

Table 4. (continued).

1964–1970		Best Estimate				Upper Limit		
Waste Stream	Estimation Bases and Assumptions	Fraction Particulate	Upper Break (µm)	Percent Particulates in Transportable Range (%)	Inventory in Transportable Range (kg)	Fraction Particulate	Percent Particulates in Transportable Range (%)	Inventory in Transportable Range (kg)
Type I Combustibles	Curies on combustible material used in support of Bldg 771 aqueous type operations (i.e., ion exchange, waste treatment, and laboratory work). Half particulate at a 20-µm upper break size (see Geldart[c] powder classification diagram).	0.50	20	2.24	0.625	0.83	3.29	1.524
Type II Noncombustibles	Curies from Bldg 771 aqueous-type operations (i.e., operations, waste treatment, and laboratory work). Half particulate at a 10-µm upper break size—due to aqueous dissolution processes (*Perry's Chemical Engineers' Handbook*[a] Section 19, "Filtration"). Some of the particulate material is probably the difficult-to-dissolve refractory form.	0.50	10	5.40	1.357	0.83	7.38	3.077
Type III HEPA on drybox operations	All curies from Bldg 776 pyro, Bldg 771 calcination, and foundry operations emissions, and all is particulate. Estimated a 45-µm upper break size using the "metallurgical dusts and fumes" line in the particulate characteristics chart (same as was done for the 1954–1963 prefilters).	1.00	45	0.80	0.594	1.00	1.24	0.916
Type V Noncombustibles outside drybox	Curies from Bldg 776 pyro and Bldg 771 calcination, from foundry operations, and remainder from research and development. Assumed 50% is from particulates; remainder is soluble plutonium form on noncombustible surfaces. Assumed the 20-µm upper break size using the Geldart[c] powder classification diagram—and assuming that decontamination practices were intensified so that only cohesive particles were left on surfaces.	0.50	20	2.24	1.414	0.83	3.29	3.445
Line-generated waste Noncombustibles inside drybox operations	Curies from Bldg 776 pyro and Bldg 771 calcination and from foundry operations. Particulate material was dispersed, settled, and adhered in and on surfaces inside drybox. Assumed 90% is from particulate emissions; remainder is soluble plutonium on surfaces. Assumed the 20-µm upper break size using the Geldart[c] powder classification diagram—and assuming that decontamination practices were intensified so that only cohesive particles were left on surfaces.	0.90	20	2.24	3.219	1.00	0.30	0.094

Table 4. (continued).

1964–1970		Best Estimate				Upper Limit		
Waste Stream	Estimation Bases and Assumptions	Fraction Particulate	Upper Break (µm)	Percent Particulates in Transportable Range (%)	Inventory in Transportable Range (kg)	Fraction Particulate	Percent Particulates in Transportable Range (%)	Inventory in Transportable Range (kg)
Graphite	Plutonium metal in graphite molds; majority of the PuO_2 formed from this material is not the difficult-to-dissolve refractory form. As before, used 100%-intercept of 735 µm from final R-R fit—but assuming intensified decontamination practices back-calculated an upper break size of 137 µm using the "old" 735-µm limit and the two graphite stream "kg per year" values (254.3 kg/9 years vs. 31.5 kg/6 years [see Figure 3]).	1.00	137	0.20	0.062	1.00	0.30	0.094
Series 741 sludge	All sludge plutonium curies are composed of the difficult-to-dissolve refractory PuO_2 form generated primarily in the Bldg 771 calcination process and any process where plutonium was "burned." This sludge is primarily from underflow from the Bldg 771 aqueous dissolution, leaching, and filtration processes. Based on *Perry's Chemical Engineer's Handbook* Section 19, "Filtration"; assumed a 3-µm upper break size.	1.00	3.0	24.85	21.837	1.00	29.04	25.517
Series 743	Same as for Series 741 sludge	1.00	3.0	24.85	0.671	1.00	29.04	0.784
Series 744	Same as for Series 741 sludge	1.00	3.0	24.85	0.777	1.00	29.04	0.907
Series 745	Same as for Series 741 sludge	1.00	3.0	24.85	0.024	1.00	29.04	0.028
	Total 1964–1970 SDA RFP plutonium in transportable range (kg) =				30.58			41.54
	Best estimate total SDA RFP plutonium in transportable range (kg) =				41.87			
	Upper limit total SDA RFP plutonium in transportable range (kg) =							55.53

a. Zodtner and Rogers 1964.
b. Geldart 1986.
c. Perry 1984.

HEPA = high-efficiency particulate air
RFP = Rocky Flats Plant
R-R = Rosin-Rammler
SDA = Subsurface Disposal Area
Z&R = Zodtner and Rogers (1964)

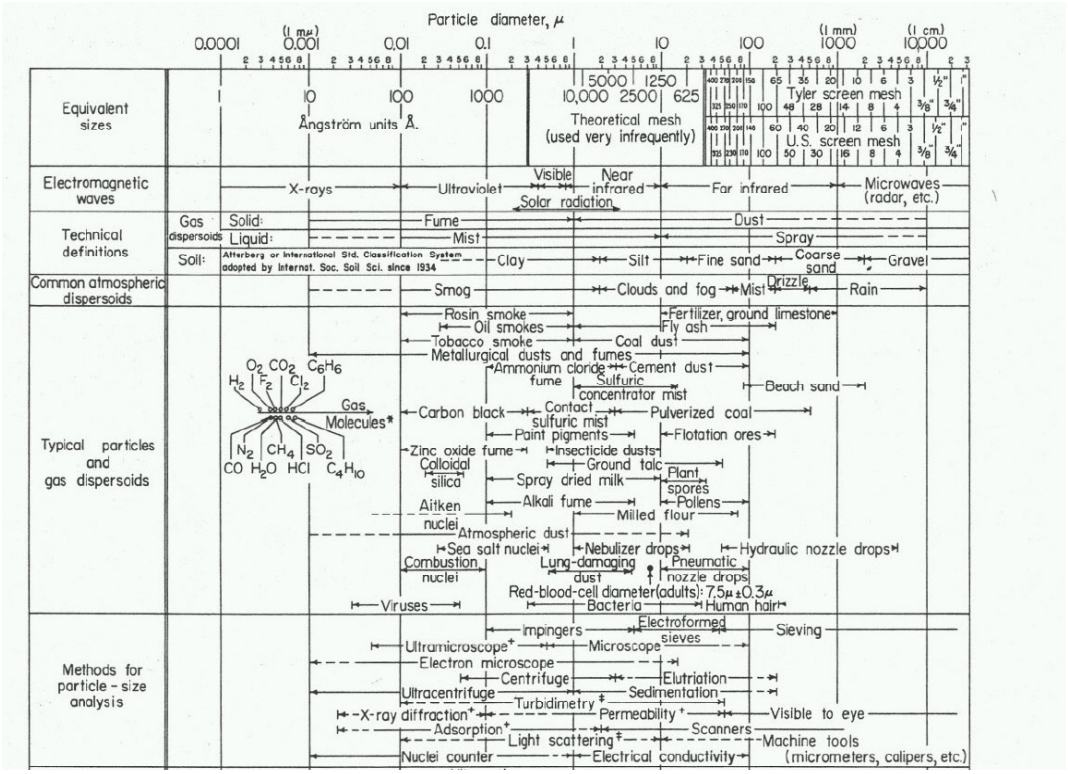

Figure 4. Excerpt from the Stanford Research Institute particle characteristics chart (Perry 1984).

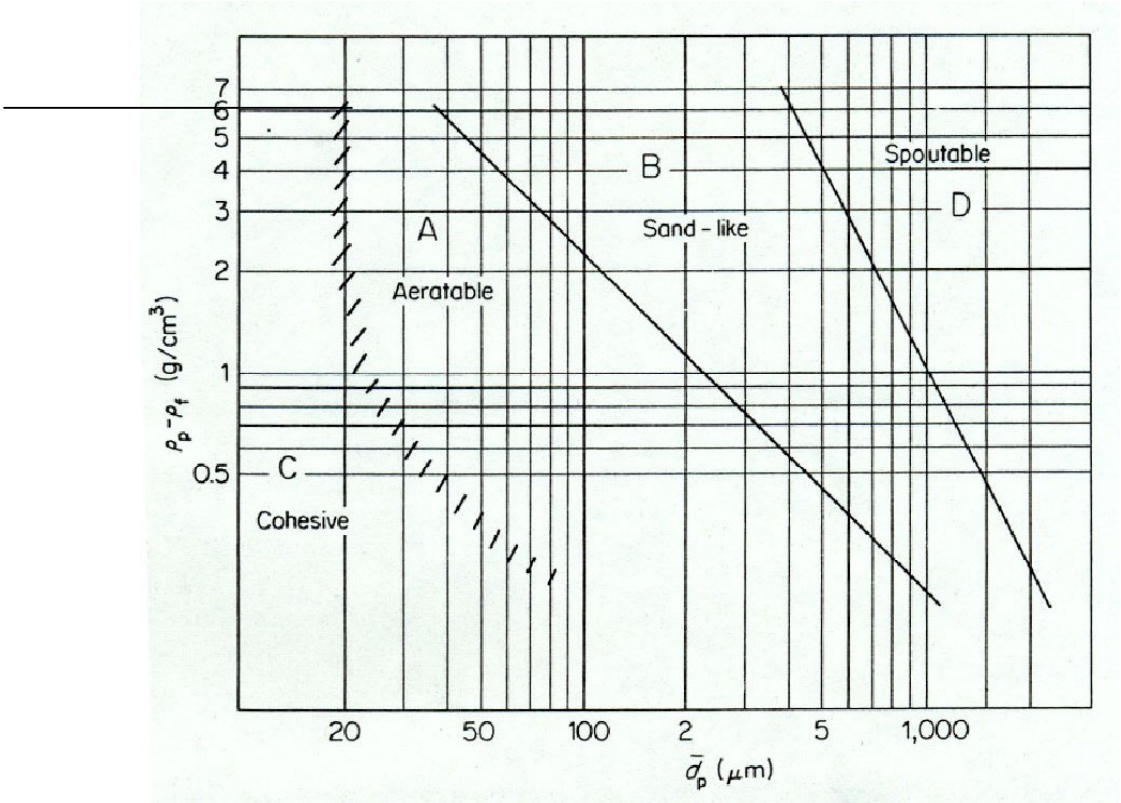

Figure 5. Geldart powder classification chart (Geldart 1986).

2.5 Calculate Percent of Transportable Colloidal Material in Waste Stream

Percent particulates in transportable-range values were calculated using Equation (2):

$$\%Transportable = 100 \times \left(\frac{CumWt\%_{1\mu m}}{CumWt\%_{upper\ break\ \mu m}} \right) \quad (2)$$

where

$CumWt\%_{particle\ size}$ is determined by inserting the particle size into the PSD equation established in Section 2.2.

The upper break size is an estimate for the upper particle size of the waste stream particulate material from which a weight-percent value is attained for the waste stream. The 1-µm size is the accepted upper break for colloids (Shaw 1980). Although 1 nm is the accepted lower size for colloids (Shaw 1980), this lower break size was not used in the numerator to bound the transportable range. A value of 1 nm also was identified in Kersting (1999) and in Section 6.6.1 of Hoffman (2002). Because of negligible weight-percent values obtained from the PSD equation for the size fraction less than 1 nm, a lower break size also was not used in the denominator to bound the waste stream. An upper break size of less than 1 µm was not used for any of the waste streams. Therefore, the relative portion (as a percent) of waste stream particulate material in the colloidal range is obtained from this expression. Because actual PSD data from waste streams do not exist, this method was used to estimate percent particulate in transportable range. Calculation results are presented in Table 4.

2.6 Calculate Amount of Transportable Colloidal Plutonium-Particulate Material in Waste Stream

Inventory in the transportable range for each waste stream was calculated as shown in Equation (3).

$$\begin{array}{c}\text{Inventory in} \\ \text{transportable} \\ \text{range (kg)}\end{array} = \begin{array}{c}\text{Fraction} \\ \text{particulate}\end{array} \times \begin{array}{c}\text{\% Particulates} \\ \text{in transportable} \\ \text{range (decimal form)}\end{array} \times \begin{array}{c}\text{Total plutonium} \\ \text{(kg)} \\ \text{(from Table 3)}\end{array} . \quad (3)$$

Estimates of plutonium mass inventory in the transportable range were calculated based on preceding discussions and assumptions presented in Table 4. These best-estimate values are presented in Table 4. Then upper-limit values were calculated, using the 95% upper confidence limits for parameters of the PSD equation, to bound the estimate of colloidal plutonium (see Section 2.7).

2.7 Assess Uncertainty

Effects of the error associated with the R-R fit of these literature data, the fraction and upper break size estimates, and use of the percent-transportable approximating expression (i.e., Equation [2]) to determine best-estimate values are smaller than the uncertainty involved with not having actual representative waste stream data. Disregarding these uncertainties, the fraction and break-size estimates were biased, where appropriate, toward a larger fraction of plutonium in the colloidal-size range.

The standard error of estimate (i.e., $s_{y/x}$) quantifies the spread around the R-R fit line (Charpa and Canale 1988) of the BARF and Curve D data. The upper-limit kilogram values of inventory

in the transportable range were obtained by adding $2 \times s_{y/x}$ to the PSD equation weight-percent value in both the denominator and numerator of the percent-transportable equation, Equation (3). These upper-limit results quantify the uncertainty of these estimates (with reference to best values) and are presented in Table 4. The $2 \times s_{y/x}$ upper-limit *cum wt%*< is shown in Figure 3. This curve represents the upper 95% confidence limit of the estimated R-R curve.

For the best estimate, a total of 41.87 kg of plutonium is in the transportable particulate range, with 11.29 kg from the 1954–1963 era and 30.58 kg from the 1964–1970 era. For the 95% upper confidence limit, a total of 55.53 kg of plutonium is in the transportable particulate range, with13.99 kg from the 1954–1963 era and 41.54 kg from the 1964–1970 era.

3. PLUTONIUM COLLOID MOBILITY

The following sections summarize an analysis of literature about potential mobility of PuO_2 colloids with special attention given to the RWMC environment. The analysis is confined to potential mobility of plutonium as PuO_2 particles. Thorough reviews of the range of factors that can affect plutonium mobility in the environment—including variations in chemical form, complexation by organic compounds, dissolution-precipitation equilibria, and facilitated transport by other colloids—can be found in other references (e.g., Flury and Harsh 2003).

Explicitly demonstrating that PuO_2 particles contribute to migration of plutonium, and calibrating models used to simulate colloid transport, requires direct measurements of PuO_2 colloids along flow paths in the vicinity of the SDA. Such data are not available. Over time, routine quarterly monitoring of the vadose zone and aquifer near the SDA has yielded only a few positive plutonium detections. These rare detections typically occurred near method-detection limits and do not exhibit trends over depth or time (Koeppen et al. 2004). Therefore, information to test candidate models for colloid transport or interpret mechanisms of transport is absent. Cleveland and Rees (1982) conducted an analysis of water samples below the Idaho Nuclear Technology and Engineering Center for the presence of Pu-238. Although filtered and unfiltered samples were analyzed, plutonium colloids in the samples were not clearly evident.[d] An analysis of plutonium in surficial sediments at the SDA (Ibrahim and Morris 1997) did detect plutonium that was strongly sorbed to other mineral phases; however, the analytical procedures were not well suited for detecting colloids. An absence of PuO_2 particles, if they ever existed, would indicate that colloid transport is at least faster than for dissolved plutonium species. (It is not clear whether sequential extraction methods used by Ibrahim and Morris [1997] would have detected particulate PuO_2.)

An analysis of groundwater and perched water beneath the SDA was conducted by Roback et al. (2000) using sensitive thermal ionization mass spectrometry. Plutonium was not detected in aquifer samples, but two perched water samples yielded positive results. The plutonium speciation in these samples (i.e., dissolved or particulate) is unknown. Without obtaining and analyzing samples from areas between the probable sources and where plutonium was detected, it is not reasonable to conclude that detected plutonium represents a contaminant plume. The potential for dislodging particulate matter during sample extraction prevents the conclusion that detected plutonium, if in particulate form, is actually mobile under ambient conditions. However, it does appear that plutonium has been transported to depth (i.e., 73 m [240 ft]) and may have originated from waste buried in the SDA.

Because direct field data are not available and because analysis in this report is in support of risk assessment, recommendations for parameters for use in simulating PuO_2 colloid transport will reflect a bias toward higher rates of migration when lower rates of transport cannot be explicitly defended.

Behavior of colloids and how colloids are transported in porous media under saturated and unsaturated conditions have been extensively covered in related literature (Roy and Dzombak 1997; Honeyman 1999; Lenhart and Saiers 2002; Saiers and Lenhart 2003). However, most of this literature reports on either general principles of colloid behavior and filtration or on observational information from specific field sites. For practical application to modeling particle transport at the SDA, and in the absence of site-specific information, it is necessary to consider the scientific knowledge base in the context of environmental characteristics of the SDA, and to draw on multiple lines of indirect information.

d. The reported activity of Pu-238 in unfiltered samples was consistently higher than in those of filtered samples; however, differences were not statistically significant. In addition, it was not clear in the report whether loss of Pu-238 by adsorption could have occurred during filtration because results from control experiments were not presented.

Practical simulations of contaminant transport frequently involve using a mass-based distribution coefficient, K_d, as shown in Equation (4).

$$Kd_i = \frac{\left(S_{i,sorbed} / M_{solid} \right)}{(C_i)} \tag{4}$$

where

K_{di} = Partition coefficient for solute i

$S_{i,sorbed}$ = Mass or activity of solute removed from solution

M_{solid} = Mass of solids in contact with solution

C_i = Dissolved concentration or activity.

Solute K_d values are determined either by directly measuring portioning of solids and solutions or by fitting laboratory or field solute transport data with effective K_d values. Experimentally determined K_d parameters generally assume (1) equilibrium or steady-state conditions, (2) that partitioning is reversible, and (3) that the proportionality between solid mass and solute adsorbed is constant. When K_d parameters are used in models to predict solute transport, these assumptions must be satisfied and the geochemical environment of the field system must be comparable to the conditions under which K_d parameters were determined. However, colloid transport is distinctly different from solute transport in several ways including the following:

- Colloids can be immobilized in porous media by both physical straining and attachment to surfaces
- Attachment and detachment cannot be modeled as an equilibrium state
- Colloid trapping (attachment or filtration) can be irreversible
- Colloids will be confined to permeable regions (e.g., large pores, preferred flow paths, and fractures)
- Diffusion of colloids is much lower than for molecular solutes.

The following sections address two main issues:

1. Potential mobility of PuO_2 colloids from plutonium source(s) to the water table in the SDA environment
2. Method by which colloid transport should be modeled, using current models, to estimate PuO_2 particle migration below the SDA.

3.1 Analysis

The following review concentrates on developing conservative estimates of plutonium transport. Excellent reviews of fundamental principles of colloid transport are available elsewhere (e.g., Elimelech et al. 1998; Flury and Harsh 2003; Ibaraki and Sudicky 1995; Roy and Dzombak 1997; and Ryan and Elimelech 1996); therefore, a general discussion on colloid transport is not provided here.

As with calculating inventory of colloidal-sized plutonium buried in the SDA (discussed in Section 2), insufficient experimental or field data are available to predict PuO_2 colloid transport. Therefore, indirect or inferential information is used in the analysis. The following subsections address each category of information in terms of the contribution of each to assessing mobility of plutonium colloids at the SDA and potential for movement specifically under conditions at the RWMC.

3.1.1 Fundamental Models

Fundamental models are used to synthesize physical and chemical principles that describe colloid mobility. While these models are scientifically defensible, they cannot be readily applied to natural field conditions because it is difficult to determine values for the model parameters that accurately represent field conditions. However, basic models do provide qualitative insight into what factors are likely to be important in determining trends in colloid mobility.

Attention to colloid-facilitated transport of contaminants over past decades has resulted in models for simulating colloid transport in porous media. Under saturated conditions, a balance between attracting and repelling forces governs the attachment strength of colloids to mineral surfaces. These forces are described generally by the DLVO[e] theory (Elimelech et al. 1998) and variations of that theory. Electrostatic interactions (attracting or repelling), dispersion forces (always attracting), and hard-shell limits to surface-to-surface contact are the primary contributors to surface-to-surface interactions. Electrostatic interactions are frequently the best predictor for whether particles (e.g., minerals and cells) will readily adhere to or be repelled by other surfaces. Effective electrostatic charge on mineral surfaces is determined by reactions with dissolved solutes that generate charged surface sites (e.g., H+, OH-, and other adsorbing solutes), fixed charge generated by substitutions in the crystal lattices, and the concentration of electrolytes that do not interact specifically with surfaces but can screen surface charge. Mineral surfaces have a net negative charge under most ambient conditions. The magnitude of each of the various forces depends on distance between surfaces as they come into contact. Even surfaces with like charges can adhere if collisions produce sufficient energy (due to thermal or physical energy) to overcome repelling electrostatic interactions and position surfaces in a primary energy minimum. In low-energy environments, surfaces can become irreversibly attached.

While DLVO-based theories provide an estimate of potential strength of binding, colloid partitioning to stationary surfaces also is determined by factors that are derived from experimental testing and model calibration (e.g., collision frequency, capture efficiency, detachment rate, and diffusion into zones of immobile water). Physical filtration also must be considered for a complete model. Physical filtration includes trapping particles in small pore throats and immobilizing particles in thin films of water in unsaturated conditions. Theoretical models describing colloid capture have been successful in simulating the general behavior of colloids in highly idealized experimental systems; however, theory generally underpredicts colloid capture, sometimes by large margins, compared to experimental data. When research goals have specifically targeted model development, experiments have frequently used simple media with mean-pore diameters greater than colloid diameters by factors of 100–1,000 to

e. DLVO is the acronym for individuals credited with the theory: Derjaguin, Landau, Verwey, and Overbeek.

minimize physical filtration and to obtain transport data within a reasonable time. Such conditions are not necessarily representative of a natural system (e.g., interbed sediments).

Early filtration theory only considered colloid attachment as an irreversible process. While theory can explain the attachment strength between colloids and collector surfaces, theories for colloid detachment have not been successful. Instead, empirical linear expressions have been used when the combination of colloid attachment and detachment were needed to describe colloids through porous media. Model parameters generally must be adjusted to establish good fits to experimental data. Most often, colloid detachment is observed to be a consequence of abrupt changes in flow or chemical conditions (Bergendahl and Grasso 1999; Loveland et al. 1996; Ryan and Gschwend 1994).

Colloid attachment (Ibaraki and Sudicky 1995) is a product of a filtration coefficient, a velocity factor, a Darcy velocity, and a dynamic blocking factor. The filtration coefficient can be theoretically derived (Yao, Habibian, and O'Melia 1971). One interesting feature of the theory for colloid transport and filtration is that maximum extent of transport occurs for colloids in a narrow size range—roughly 1–2 μ in diameter. Smaller particles, rather than being more mobile, have sufficient energy to overcome repelling surface-to-surface interactions and can become strongly attached to collector surfaces. Settling and physical straining traps larger particles. Attachment between surfaces has been found to be irreversible in the absence of significant physical or chemical perturbations.

Treating INEEL interbed sediments as packed-bed granular filters, the distance of colloid travel within interbeds can be calculated from semitheoretical models used to simulate performance of granular filter beds. (See Appendix A for details about the calculations and parameters.) A filtration efficiency factor that appears in calculations, α, must be determined empirically. A value of $\alpha = 1$ means collisions between colloids and sediment grains always result in attachment (i.e., conditions for filtration are highly favorable). A value of $\alpha = 0.001$ represents conditions unfavorable for filtration (i.e., 99.9% of colloid-grain collisions do not result in attachment). In experimental measurements of α under conditions that have been intentionally set to be unfavorable for colloid transport—where colloids and packed media had similar (i.e., repelling) surface charges and the solution had low ionic strength (Elimelech and O'Melia 1999)—α values were greater than 0.001. In calculation results that follow, a more extreme value of $\alpha = 0.00001$ was used to simulate conditions that are more unfavorable for colloid capture than has been experimentally observed in column studies where unfavorable conditions are established. Other parameters for the calculations are listed below:

- Colloid diameter = 0.001 mm (a size near the optimal range for transport)
- Colloid density = 11.4 gm/cm^3
- Sediment porosity = 0.40
- Flow = 10 cm/year (range is 1–10 cm/year and higher velocities enhance colloid transport)
- Mean grain size = 0.5 mm (Huges 1993).

These parameters are for Case 1. For comparison, parameters that fall outside the range for C-D interbed material and that will result in higher rates of colloid transport were also tested and are called Case 2. Parameters for Case 2 are

- Porosity = 0.50
- Flow rate = 100 cm/year
- Grain size = 2 mm.

In both cases, the temperature is 10°C.

The calculated travel distances through a porous medium where 99.999% of colloids are removed ($C_1/C_0 = 0.0001$, see Appendix A) are:

- Case 1 = 4.7 cm
- Case 2 = 205 cm.

In addition to the high filtration efficiency predicted by theoretical calculations, several additional issues should be considered. Theories were developed for smooth, uniform, and spherical collector grains and colloids. Real materials are characterized by surface roughness and patchy distributions of surface attachment sites. These factors have been invoked to explain how colloid adsorption and capture observed in experiments generally exceed theoretical predictions during unfavorable filtration conditions In addition, the calculations used an efficiency parameter value (i.e., 0.00001) that is much lower than observed during experiments for unfavorable filtration conditions.

These calculations indicate that colloids should not be mobile under conditions in interbeds beneath the SDA. Mobile colloids are observed in nature; however, in contrast to laboratory experiments designed to maximize colloid mobility, natural colloid mobility appears generally to be associated with perturbations in physical (flow) and chemical (changes in ionic strength) conditions. In addition, colloids measured in groundwater frequently can be artifacts of sampling methods. Current theory does not explain the impact of such perturbations on detachment of colloids; therefore, an important assumption in calculations described above is that physical and chemical conditions are constant to achieve such low colloid mobility.

While development of models for predicting colloid transport has progressed, gaps in knowledge make it difficult in this case to apply existing models to the question of PuO_2 transport. Conditions that impact colloid stability and reduce transport are

- Size (colloids in the 0.1–2-μ range are theoretically more likely to be transported depending on pore structure of the porous media)
- Net surface charge of colloids and stationary surfaces
- Ionic strength (high concentrations of dissolved salts [generally above 0.05M]) will reduce electrostatic repulsion between surfaces.

One significant knowledge gap concerns surface chemical properties for $PuO_2(s)$ and relationships between surface charge and system conditions. Published data that describe the dependence of PuO_2 surface charge on system conditions (e.g., pH and ionic strength) are not available. However, net surface charge still appears to be a reasonable qualitative predictor of colloid stability and mobility in the subsurface. With respect to PuO_2 colloid transport, the recommended assumption is that PuO_2 has a net negative charge and that colloid stability and transport will be favorable. Fundamental filtration theories predict that all colloids are eventually immobilized. This is not consistent with many field observations

where colloid mobility may be due to physical and chemical perturbations. Many factors influence colloid capture and release in porous media, and is it difficult to draw simple analogies to that transport of solutes. In particular, the reversibility of colloid attachment cannot be predicted. Some of the most important factors determining colloid mobility, particularly in the near-surface environment of the SDA, may be temporal variability in physical and chemical conditions—topics that basic theories do not address.

3.1.2 Physical Experiments

Physical experiments are conducted under controlled laboratory conditions using idealized packed media or media representative of sites of interest. The majority of such published experiments have been used to test fundamental models, and these controlled conditions are generally oversimplified compared to complex natural environments. However, some laboratory studies have replicated aspects of field conditions relevant to the SDA.

Important characteristics of water infiltrating an unsaturated system are

- Presence of an air-to-water interface
- Shear forces
- Disruptive energy associated with water advance driven by capillary forces.

An advancing air-to-water interface is important for two reasons:

1. The interface provides a mobile surface to which colloids may attach, particularly colloids with dehydrated surfaces that are at least temporarily hydrophobic
2. Energy associated with capillary-driven intrusion into pores can dislodge particles attached to surfaces.

Episodic infiltration of water should facilitate rapid transport of at least a fraction of colloidal materials in the near-surface environment of the SDA. An INEEL-supported study at Clemson University (Fjeld, Coates, and Elzerman 2000) shows rapid movement of a small fraction of actinides in column tests with SDA soil. Plutonium-spiked tracer solutions were introduced into dry soil columns, mimicking infiltration of precipitation into dry SDA soil. Appearance of a fraction of high-mobility actinides in column effluent, eluting in less than one pore volume, strongly suggests transport of solids on an advancing air-to-water interface. Though the study involved dissolved actinide species, the amount of material mobilized in the fast fraction was a very small fraction of the total applied to the columns. Colloid transport was either as intrinsic colloids formed in the column or as actinides attached to colloidal material already present in the column.

Additional studies also have shown evidence for high mobility fractions of actinides, including plutonium, in a rock block (Fried, Friedman, and Weeber 1974) and in a column of crushed tuff (Thompson 1989). An important observation is that high-mobility fractions are separated from low-mobility fractions. Therefore, the total population of plutonium cannot be represented as a simple

continuous solute or colloid plume. While colloid-facilitated transport is implicated, colloids were not directly observed—only inferred.[f]

Recent studies (Lenhart and Saiers 2002; Saiers and Lenhart 2003) illustrate how colloids can be mobilized during infiltration events in unsaturated packed columns of silica sand. Although shear forces and the air-to-water interface were operable in these reports, a proposed quantitative model did not describe the mobilization processes explicitly. However, mobilization of colloids was found to be correlated to the strength of attachment and to the fraction of surfaces exposed to water as the rate of infiltrating water increases. Shear and capillary forces are important in detaching colloids that are attached with mineral surfaces by weak electrostatic interactions when the colloid diameter is greater than the thickness of a stationary boundary layer.

A study by Gamerdinger and Kaplan (2001) illustrated the effect of variations in ionic strength and flow velocity on transport of latex colloids in quartz sand and Yucca Mountain tuff under unsaturated conditions. As expected, colloid retention was shown to increase when flow velocity (Darcy velocity) decreased and ionic strength increased. In all cases, at least a fraction of the latex particles passed entirely through the columns. However, a critical point is that these experiments, as is true for nearly all laboratory colloid-transport experiments, were conducted under very high flow rates compared to natural systems. Flow in interbeds under the SDA measures 1–10 cm/year (Magnuson and Sondrup 1998). In the Gamerdinger study, a centrifuge was used to increase flow rates to 22,000–44,000 cm/year. Trends in colloid deposition still were seen even though flow rates were high. The explanation for observed trends includes both ionic-strength effects (higher attachment rates for higher ionic strengths) and higher colloid retention in zones of low fluid mobility.

The most important conclusion from laboratory studies involving PuO_2 colloids, and colloids in general, is that a small high-mobility fraction of plutonium is often observed, that this high mobility fraction can be physically separated from the low mobility fraction, and that the high mobility fraction is most likely associated with mobile colloids. The higher mobility can be based on particle size, speciation (i.e., soluble vs. colloidal), filtration kinetics (e.g., attachment, detachment, site blocking, or physical straining), or other mechanisms (e.g., shear forces in preferred flow paths or concentration of particles on advancing air-to-water interfaces). Laboratory studies often are conducted under conditions that would, in the natural world, represent transitional states (e.g., transitions to high flow or low ionic strength). Although the relationship between laboratory and field conditions could be considered limited, laboratory studies do point out the importance of physical and chemical transitions for increasing colloid mobility.

3.1.3 Simplified Conceptual Field-scale Models

Simplified conceptual models have been applied to Yucca Mountain field test sites where some monitoring data make it possible to extract effective parameters for models. Though the Yucca Mountain Project conceptual model is not necessarily appropriate for the SDA, some similarities are relevant.

The colloid transport model used for the Yucca Mountain Project (Moridis et al. 2003) used simple linear expressions to describe kinetics for both colloid attachment and detachment. Parameters were derived semitheoretically for colloid attachment and from inverse modeling. No particular basis was given for expressing colloid detachment with a linear correlation to surface concentrations; however, the model makes it possible to simulate colloid transport in a way that is somewhat analogous to solute transport where sorption is reversible and long-range transport is possible. In keeping with current

f. One dilemma with respect to identification of colloids is that analytical methods are not available. Reliance is largely on operational definitions based on filtration procedures that will not capture a large fraction of colloids below a cut-off point.

filtration theory, the attachment expression (Ibaraki and Sudicky 1995) is a product of a filtration coefficient, a velocity factor, the Darcy velocity, and a dynamic blocking factor. A filtration coefficient for the SDA could be theoretically derived in the same way (Yao, Habibian, and O'Melia 1971).

Conceptual elements of the Yucca Mountain Project model approach cannot be readily incorporated into the existing transport model used for the SDA (i.e., TETRAD). Complex modifications would have to be considered, including how sorption and desorption are kinetically controlled (not determined by equilibrium conditions), how colloid diffusion is much lower than for solutes, and how colloid migration paths depend on colloid size. A number of parameters in the SDA model (e.g., the kinetic constants for attachment or detachment, diffusion, and physical filtration) can be estimated from theoretical principles, although field conditions are not sufficiently characterized and uncertainty in parameterization would be high. Model calibration may be impossible without field data for colloid concentrations and migration over time.

The SDA system is significantly different from the Yucca Mountain Project system in a number of ways—specifically with respect to episodic flow. Application of the Yucca Mountain Project model to the SDA system would require an evaluation of the parameterization. An important point illustrated in the Yucca Mountain model simulations reported by Moridis et al. (2003) is that large particles are transported more rapidly than small particles because large particles are confined to larger pore spaces, faster flow paths, and fractures. With respect to applications to the SDA environment, the Yucca Mountain model is more appropriate for steady-state conditions; whereas, the near-surface environment of the SDA experiences episodic infiltration events likely to include transitions in solution chemistry. Steady state conditions are more likely to exist at depth below the SDA; however, to apply the Yucca Mountain colloid transport model, it is necessary to calibrate or parameterize the model against colloid transport observed in the field.

3.1.4 Analogous Sites

The best evidence for PuO_2 transport obviously would come from field studies at the SDA. Alternatively, sites with environmental conditions that are well matched to those of the SDA can be used. Drawing analogies between possible colloid transport at the SDA and colloid transport at other sites requires demonstrating a high degree of similarity between the study site and the site of interest (i.e., the SDA) in terms of the physical, chemical, and biological environment and the nature of the contaminant (i.e., colloidal PuO_2). In this analysis, the most important features may be (1) the unsaturated conditions and (2) that infiltration of water occurs during relatively brief events.

In general, field studies have shown that plutonium migration in subsurface environments is extremely slow, largely because plutonium binds strongly to most mineral and organic surfaces in the subsurface. However, a well-known study at the Nevada Test Site (Kersting et al. 1999) has been frequently cited as evidence for processes that can result in rapid migration of plutonium, which in this case originated from an underground weapon test.[g] Fracture flow and unusual forces associated with a bomb test arguably can accelerate movement of dissolved plutonium, though most of the transported plutonium appears to have been associated with aluminosilicate colloids (rather than as PuO_2). Plutonium concentrations in water collected at the Nevada Test Site are high. Laboratory studies of colloid transport where colloid concentrations are high have shown that high concentrations of adsorbed colloids can

g. Radionuclide pseudocolloids were detected in a well 300 m southwest of the underground detonation site. In 1996, plutonium concentrations of up to 0.63 pCi/L were detected at Well ER-20-5. Almost all plutonium was associated with colloids composed of silica, zeolites, and clays. The ratio of Pu-239 to Pu-240 indicated that plutonium originated from the Benham nuclear test, which was conducted in December 1968 approximately 1.3 km (0.8 mi) from Well ER-20-5. Thus, plutonium traveled more than 1 km (0.6 mi) in less than 30 years.

inhibit further attachment of colloids (Ryan and Elimelech 1996; Loveland et al. 2003). This "blocking effect" will further enhance colloid migration.

In contrast, Litaor et al. (1998) indicated that plutonium-particle migration at RFP has not been significant. The RFP is an important site because, like the SDA, the environment is arid and infiltration is from sporadic rain and snowmelt. Penrose et al. (1990) suggested that plutonium isotope transport at Mortandad Canyon at the Los Alamos National Laboratory is extremely rapid based on samples taken from wells along the groundwater gradient. However, a recent analysis (Marty, Bennett, and Thullen 1997) of the Penrose report showed that groundwater transport could not have accounted for plutonium migration, and that surface transport and contamination of wells from surface runoff was a more likely explanation.

In a recent report by Laue and Smith (2004) a radiographic technique was used to measure the downward migration of plutonium in the near-surface environment of Plutonium Valley at the Nevada Test Site. At Plutonium Valley, a surface test was conducted in the 1960s where nuclear weapons were destroyed using conventional explosives. This test resulted in deposition of plutonium-containing aerosols on the desert floor. Presumably, based on the strength of binding of plutonium species to soil components, the expectation was that downward migration would be minimal. However, radiographic evidence indicates that migration (at least 40 cm [16 in.] in 40 years) exceeded expectations based on the strong sorption of plutonium found for most soils. The migration of plutonium possibly was due to the movement of particles containing plutonium along preferential flow paths (e.g., near plant roots). This conclusion is significant because the arid environment of Plutonium Valley is similar to that of the INEEL. Although the migration rate may not appear to be rapid, the net infiltration of water in arid environments is generally near zero due to evapotranspiration. Localized ponding or flood events can be a mechanism for transporting colloids deeper than the average regional infiltration depths.

3.2 Results from Ancillary Information

Questions about PuO_2 mobility at the INEEL is limited because of the following:

- Use of theoretical predictions is limited
- Appropriate laboratory studies are few
- Field data that can be used to test or calibrate possible colloid transport models are not sufficient
- A good match to specific SDA site characteristics has not been studied.

However, insight can be derived from a combination of the four analytical approaches. If plutonium is present as a range of PuO_2 colloids (see earlier sections), and water infiltration is episodic and potentially rapid at times, existing evidence from laboratory and field studies indicates that at least a fraction of PuO_2 less than 1 μ in size could be highly mobile. This conclusion is based on (1) the physical impact of water infiltrating through intermittently unsaturated (especially dry) media, (2) physical heterogeneity and fast flow paths in environmental media, and (3) low ionic strength of infiltrating water. Therefore, most evidence points to the importance of transitions in physical and chemical conditions for promoting mobilization of PuO_2 colloids.

The near-surface conditions at the SDA (i.e., episodic flow of low-ionic-strength water) seem well suited to promoting migration of a fraction of PuO_2 colloids if they are present. Episodic infiltration can carry colloids at advancing air-to-water interfaces. Shear forces can overcome electrostatic attractions if flooding events occur and fast flow paths are present, though nonlaminar flow is not expected in surficial

sediments even during flood events. Shear forces, however, may not be significant in surficial sediments at the SDA because the soil is relatively homogeneous, and flow probably does not occur along fractures or fast flow paths even during flood events. Infiltrating water also is likely to have low concentrations of dissolved ions (low ionic strength), further enhancing the repulsive interactions between surfaces with like charges. Repulsive interactions are consistent with DLVO theory and the assumption that PuO_2 surfaces are similar to other mineral oxide phases with respect to pH-dependent surface-charge development. Mobilization in response to changes in solution chemistry has been well documented, though it has not been rigorously described in theory (McDowell-Boyer 1992).

Deeper subsurface conditions (e.g., dissipated energy, low flow rate, saturated conditions, or higher ionic strength) favor immobility. Conditions where particle attachment is maximized and remobilization is minimal include steady laminar flow, constant saturation state, and constant chemical composition at depth at the SDA (McElroy and Hubbell 2004; McDowell-Boyer 1992). At depth, PuO_2 colloids would be trapped at locations with the appropriate conditions (e.g., in the upper section on a sedimentary interbed). With respect to modeling potential transport or interpreting field data, the distribution between sources for PuO_2 and an accumulation zone may not be well represented by a plume model for adsorbing solutes because the leading edge of the plume could have higher concentrations. Though direct field evidence for PuO_2 colloid migration at the SDA is not available, the nature of colloid transport (as described above) may result in a spatially discontinuous distribution of very small amounts of plutonium in the subsurface that could go unnoticed, depending on how sampling is conducted.

4. SUMMARY AND RECOMMENDATION

An estimate of inventory, potential mobility, and recommendations for transport-modeling parameters for colloidal plutonium were completed to provide a basis for risk assessment associated with colloidal plutonium buried in the SDA. It is estimated that about 3.7% (41.9 kg) of plutonium in shipments from RFP are in a particle-size range less than 1 μm and could migrate as colloids. Evaluation of the statistical uncertainties provides an upper-bound estimate of 4.9% (55.5 kg) of colloid-size plutonium. A review of current literature on colloidal transport is summarized to analyze potential for colloidal PuO_2 to be mobilized by infiltrating water under geochemical and hydrological conditions expected for the SDA. For release from buried waste and migration through surficial sediments and all basalt units, a K_d of 0 mL/g is recommended for the estimated colloidal plutonium fraction. This reflects the potential mobility of colloids in high flow velocity, low ionic-strength regimes, which could exist during flooding or snowmelt in the SDA. High flow velocities would persist as water moved down through fractured basalt. Once percolating water encounters a sedimentary interbed, flow velocity will decrease and ionic strength will increase. Under these hydrochemical conditions, colloids will be filtered out of percolation and will sorb to interbeds. Because no mechanism is available to create high flow velocities in interbeds, this colloidal plutonium, once sorbed, will not be remobilized in colloidal form. The mechanism for remobilization of this plutonium will be dissolution and transport in the dissolved phase. For release and subsequent transport of this plutonium from interbeds, the dissolved-phase plutonium K_d of approximately 2,500 mL/g should be used.

4.1 Inventory Estimate

For the best estimate, a total of 41.87 kg of plutonium is in the transportable particulate range, with 11.29 kg from the 1954–1963 era and 30.58 kg from the 1964–1970 era. For the 95% upper confidence limit, a total of 55.53 kg of plutonium is in the transportable particulate range, with 13.99 kg from the 1954–1963 era and 41.54 kg from the 1964–1970 era.

A substantial amount of the plutonium-particulate material in the transportable range is associated with sludge from RFP Bldg 771 dissolution, leaching, and filtration operations. Amounts estimated in this report represent the unaffected particulate distribution at the time of disposal for the eras presented. Processes that could change particle size after burial (e.g., dissolution, leaching, or breakage) were not evaluated.

4.2 Potential Mobility

Though a small fraction of the plutonium inventory in the SDA could be colloidal particles, the vadose zone effectively captures plutonium released from the waste and migrating downward. Plutonium oxide will probably accumulate in interbeds where both hydraulic flow velocity and pore size decrease under the following conditions:

- Water is intercepted by sedimentary interbeds
- Flow through interbeds is constant and homogeneous (no fast flow paths or rapid perturbations)
- Chemical conditions are constant and reflect equilibration with the deeper geochemical environment.

Without physical or chemical perturbations, PuO_2 would be effectively immobilized in interbeds. Transport velocities in the absence of significant perturbations in flow rates or saturation of interbed are

unlikely to be sufficient to re-entrain particulate plutonium from interbeds (McElroy and Hubbell 2004); therefore, plutonium release and transport from interbeds should be treated using the dissolved-phase aqueous transport model for plutonium. Subsequent transport of plutonium would occur by dissolution of PuO_2 and migration of soluble plutonium species. Therefore, the same K_d used for transport of soluble plutonium in interbed material should be used for remobilization of the colloidal fraction and transport as part of the dissolved fraction. In some locations, the geologic model of the SDA subsurface includes gaps in interbeds. Where water flows through these gaps, colloidal plutonium will not be retained, thus allowing plutonium colloids to migrate deeper in the vadose zone to accumulate in deeper sediments.

One implication of the mechanisms by which colloids are transported is that the possible distribution of colloidal plutonium under the SDA is not be well represented by a continuous plume. Depending on the extent and duration of surface infiltration events, mobile PuO_2 may be swept through near-surface sediments (or transported to the extent of an episodic infiltration event) and then will accumulate in low-energy environments deeper in the subsurface (e.g., the interbeds). This scenario is not readily confirmed because verification depends on determining actual flow paths and whether routes (e.g., fractures) exist through which water can bypass sedimentary interbeds.

4.3 Recommendations for Modeling

Inventory estimates and transport properties developed in preceding sections will be used in the future RI/FS for OU 7-13/14 to evaluate risk associated with the SDA. Modeling for OU 7-13/14 includes source-release modeling (i.e., contaminant migration from buried waste into the vadose zone) and transport (i.e., contaminant migration within the vadose zone and aquifer). The recommendation for modeling is to assume—in the absence of additional information (e.g., parameterization or field evidence)—a K_d of zero for the estimated colloidal-size fraction (i.e., colloids less than 1 μ in diameter) of plutonium in the waste, surficial sediments, and fractured basalt, and a Kd of 2,500 (mL/g) for interbeds.

For source-release modeling, the same approach as used in the past (Becker et al. 1998; Holdren et al. 2002), with slight modifications to accommodate use of two K_ds for plutonium, is recommended for modeling contaminant migration from buried waste into the vadose zone. As in previous modeling, release rates would account both for the time of disposal and the predicted drum failure. Simulations would incorporate the bounding assumption that all mass is available for release as soon as drum failure occurs, even though much of the plutonium is in cemented sludge. Surface washoff and flux into the vadose zone would be simulated for two separate plutonium source terms: a small, mobile fraction with a zero K_d and a large, nearly immobile fraction with a K_d of 2,500 mL/g.

For transport modeling, a $K_d = 0$ mL/g should be used for fast infiltration pathways (e.g., basalt fractures), and small PuO_2 accumulation zones should be specified where infiltration is through deep sedimentary interbeds. The low energy and constant composition (e.g., higher ionic strength) conditions of such accumulation zones indicate that filtration of PuO_2 will be irreversible. Therefore, a K_d of 2,500 mL/g should be applied to accumulated plutonium in interbeds to simulate transport as a dissolved-phase contaminant.

5. REFERENCES

42 USC § 9601 et seq., 1980, "Comprehensive Environmental Response, Compensation and Liability Act of 1980 (CERCLA/Superfund)," *United States Code.*

Allen, T., 1990, *Particle Size Measurement*, ISBN: 0-412-35070-X, New York: Chapman and Hall.

Baldwin, C. E. and J. D. Navratil, 1983, "Plutonium Process Chemistry at RFP," in *Plutonium Chemistry*, ACS Symposium Series 216, W. T. Carnall and G. R. Choppin, eds., American Chemical Society.

Becker, B. H., J. D. Burgess, K. J. Holdren, D. K. Jorgensen, S. O. Magnuson, and A. J. Sondrup, 1998, *Interim Risk Assessment and Contaminant Screening for the Waste Area Group 7 Remedial Investigation*, DOE/ID-10569, Rev. 0, U.S. Department of Energy Idaho Operations Office, August 1998.

Behrens, R. G., E. C. Buck, N. L. Dietz, J. K. Bates, E. VanDeventer, and D. J. Chaiko, 1995, *Characterization of Plutonium-Bearing Wastes by Chemical Analysis and Analytical Electron Microscopy*, ANL-95/035, Argonne National Laboratory.

Benedict, M., T. H. Pigford, and H. W. Levi, 1981, *Nuclear Chemical Engineering*, New York: McGraw-Hill.

Bergendahl, J. and D. Grasso, 1999, "Prediction of Colloid Detachment in a Model Porous Media: Thermodynamics. *AICHE Journal*, Vol. 45, No.3, pp. 475–484.

Charpa, S. C. and R. P. Canale, 1988, *Numerical Methods for Engineers*, 2nd Edition, New York: McGraw-Hill.

Cleveland, J. M. and T. F. Rees, 1982, "Characterization of Plutonium in Groundwater near the Idaho Chemical Processing Plant," *Environmental Science and Technology*, Vol. 16, No. 7, pp. 437-439.

DOE-HDBK-3010-94, 1994, "Airborne Release Fractions/Rates and Respirable Fractions for Non-Reactor Nuclear Facilities," *Vol. I – Analysis of Experimental Data*, U.S. Department of Energy.

DOE-ID, 1991, *Federal Facility Agreement and Consent Order for the Idaho National Engineering Laboratory,* Administrative Docket No. 1088-06-29-120, U.S. Department of Energy Idaho Operations Office; U.S. Environmental Protection Agency, Region 10; Idaho Department of Health and Welfare.

Elimelech, M. and C. R. O'Melia, 1999, "Effect of Particle Size on Collision Efficiency in the Disposition of Brownian Particles with Electrostatic Energy Barriers," *Langmuir*, Vol. 6, No. 6, pp. 1153–1163.

Elimelech, Menachem, Jia Xiadong, John Gregory, and Richard A. Williams, 1998, *Particle Deposition & Aggregation: Measurement, Modelling and Simulation*, ISBN: 0-07507-7024-X, Woburn, Massachusetts: Butterworth-Heinemann, p. 440.

EPA, 1998, *Compilation of Air Pollutant Emission Factors, AP-42*, *Volume I: Stationary Point and Area Sources,* Fifth Edition, U.S. Environmental Protection Agency, URL: http:www.epa.gov/ttn/chief/ap42/, Web Page last visited April 16, 2004.

Fjeld, R. A., J. T. Coates, and A. W. Elzerman, 2000, *Final Report, Column Tests to Study the Transport of Plutonium and Other Radionuclides in Sedimentary Interbed at INEEL*, INEEL/EXT-01-00763, Rev. 0, Clemson University, Department of Environmental Engineering and Science, Clemson, South Carolina, for the Idaho National Engineering and Environmental Laboratory.

Flury, Marcus and James B. Harsh, 2003, *Fate and Transport of Plutonium and Americium in the Subsurface of OU 7-13/14*, INEEL/EXT-03-00558, Rev. 0, Idaho National Engineering and Environmental Laboratory.

Fried, S., A. M. Friedman, and R. Weeber, 1974, *Studies of the Behavior of Plutonium and Americium in the Lithosphere,* ANL-8096, Los Alamos National Laboratory.

Gamerdinger, A. P. and D. I. Kaplan, 2001, "Physical and Chemical Determinants of Colloid Transport and Deposition in Water-unsaturated Sand and Yucca Mountain Tuff Material," *Environmental Science and Technology*, Vol. 35, No. 12, pp. 2497–2504.

Geldart, D., 1986, *Gas Fluidization Technology*, Chichester, England: John Wiley & Sons.

Glover, P. A., F. J. Miner, and W. O. Polzer, 1976, "Plutonium and Americium Behavior in the Soil/Water Environment, I., 'Sorption of Plutonium and Americium by Soils,'" *Proceedings of Actinide-Sediment Reactions Working Meeting, Seattle, Washington*, BNWL-2117, pp. 225–254, Battelle Pacific Northwest Laboratories, Richland, Washington.

Hoffman, D. C., 2002, *Advances in Plutonium Chemistry 1967–2000*, American Nuclear Society.

Holdren, K. Jean and Barbara J. Broomfield, 2003, *Second Revision to the Scope of Work for the Operable Unit 7-13/14 Waste Area Group 7 Comprehensive Remedial Investigation/Feasibility Study*, INEL-95/0253, Rev. 2, Idaho National Engineering and Environmental Laboratory.

Holdren, K. Jean, Bruce H. Becker, Nancy L. Hampton, L. Don Koeppen, Swen O. Magnuson, T. J. Meyer, Gail L. Olson, and A. Jeffrey Sondrup, 2002, *Ancillary Basis for Risk Analysis of the Subsurface Disposal Area,* INEEL/EXT-02-01125, Rev. 0, Idaho National Engineering and Environmental Laboratory.

Honeyman, B. D., 1999, "Geochemistry - Colloidal Culprits in Contamination," *Nature*, January 1999, Vol. 397, No. 6714, pp. 23–24.

Huges, J. D., 1993, *Analysis of Characteristics of Sedimentary Interbeds at the Radioactive Waste Management Complex, Idaho National Engineering Laboratory, Idaho*, M.S. Thesis, Idaho State University, Pocatello, Idaho, p. 74.

Ibaraki, M. and E. A. Sudicky, 1995, "Colloid-facilitated Contaminant Transport in Discretely Fractured Porous Media .1. Numerical Formulation and Sensitivity Analysis," *Water Resources Research*, Vol. 31, No. 12, pp. 2945–2960.

Ibrahim, S. A. and R. C. Morris, 1997, "Distribution of plutonium among soil phases near a Subsurface Disposal Area in Southeastern Idaho, USA," *Journal of Radioanalytical and Nuclear Chemistry,* Vol. 226, No. 1-2, pp. 217–220.

INEEL, 2003*, Acceptable Knowledge Document for INEL Stored Transuranic Waste—Rocky Flats Plant Waste*, INEL-96/0280, Rev. 3, Idaho National Engineering and Environmental Laboratory.

Jandel Scientific, 2004, "TableCurve2D," Version 4, Jandel Scientific, San Rafael, California.

Kersting, A. B., D. W. Efurd, D. L. Finnegan, D. J. Rokop, D. K. Smith, and J. L. Thompson, 1999, "Migration of Plutonium in Ground Water at the Nevada Test Site," *Nature*, January 1999, Vol. 397, No. 6714, pp. 56-59.

Koeppen, L. Don, Alva M. Parsons, A. Jeffrey Sondrup, Paul D. Ritter, and Gail L. Olson, 2004, *Fiscal Year 2003 Environmental Monitoring Report for the Radioactive Waste Management Complex*, ICP/EXT-04-00259, Rev. 0, Idaho Completion Project.

Laue, C. A. and D. K. Smith, 2004, "Alpha-Autoradiography: A Simple Method to Monitor the Migration of Alpha-Emitters in the Environment," *Radioanalytical Methods in Interdisciplinary Research,* C. A. Laue and K. L. Nash, eds., Washington, D.C.: American Chemical Society.

Lenhart, J. J. and J. E. Saiers, 2002, "Transport of Silica Colloids through Unsaturated Porous Media: Experimental Results and Model Comparisons," *Environmental Science & Technology*, Vol. 36, No. 4, pp. 769–777.

Litaor, M. I., G. Barth, E. M. Zika, G. Litus, J. Moffitt, and H. Daniels, 1998, "The Behavior of Radionuclides in the Soils of RFP, Colorado," *Journal of Environmental Radioactivity*, Vol. 38, No. 1, pp. 17–46.

Loveland, J. P., S. Bhattacharjee, J. N. Ryan, and M. Elimelech, 2003, "Colloid Transport in a Geochemically Heterogeneous Porous Medium: Aquifer Tank Experiment and Modeling," *Journal of Contaminant Hydrology*, Vol. 65, No. 3-4, pp. 161–182.

Loveland, J. P., J. N. Ryan, G. L. Amy, and R. W. Harvey, 1996, "The Reversibility of Virus Attachment to Mineral Surfaces," *Colloids and Surfaces a-Physicochemical and Engineering Aspects*, Vol. 107, pp. 205–221.

Magnuson, S. O. and A. J. Sondrup, 1998, *Development, Calibration, and Predictive Results of a Simulator for Subsurface Pathway Fate and Transport of Aqueous- and Gaseous-Phase Contaminants in the Subsurface Disposal Area at the Idaho National Engineering and Environmental Laboratory*, INEEL/EXT-97-00609, Rev. 0, Idaho National Engineering and Environmental Laboratory.

Marty, R. C., D. Bennett, and P. Thullen, 1997, "Mechanism of Plutonium Transport in a Shallow Aquifer in Mortandad Canyon, Los Alamos National Laboratory, New Mexico," *Environmental Science & Technology*, Vol. 31, No. 7, pp. 2020–2027.

McDowell-Boyer, L. M., 1992, "Chemical Mobilization of Micron-Sized Particles in Saturated Porous Media Under Steady Flow Conditions," *Environmental Science and Technology*, Vol. 26, pp. 586–593.

McElroy, D. L. and J. M. Hubbell, 2004, "Evaluation of the Conceptual Flow Model for a Deep Vadose Zone System Using Advanced Tensiometers," *Vadose Zone Journal*, Vol. 3, pp. 170–182.

Moridis, G. J., Q. Hu, Y.-S. Wu, and G. S. Bodvarsson, 2003, "Preliminary 3-D Site-scale Studies of Radioactive Colloid Transport in the Unsaturated Zone at Yucca Mountain, Nevada," *Journal of Contaminant Hydrology*, Vol. 60, No. 3-4, pp. 251–286.

Nyhan, J. W., B. J. Drennon, W. V. Abeele, M. L. Wheeler, W. D. Purtymun, G. Trujillo, W. J. Herrera and J. W. Booth, 1985, "Distribution of Plutonium and Americium Beneath a 33-Year-Old Liquid Waste Disposal Site," *Journal of Environmental Quality*, Vol. 14, No. 4, pp. 501–509.

Orlandini, K. A., R. W. Penrose, B. R. Harvey, M. B. Lovett, and M. W. Findlay, 1990, "Colloidal Behavior of Actinides in an Oligotrophic Lake," *Environmental Science Technology*, Vol. 24, pp. 706-712.

Penrose, W. R., W. L. Polzer, E. H. Essington, D. M. Nelson, and K. A. Orlandini, 1990, "Mobility of Plutonium and Americium through a Shallow Aquifer in a Semiarid Region," *Environmental Science & Technology*, Vol. 24, No. 2, pp. 228–234.

Perry, R. H., 1984, *Perry's Chemical Engineers' Handbook*, 6th Edition, New York: McGraw Hill.

Roback, Robert C., Deward W. Efurd, Michael T. Murrell, Robert E. Steiner, and Clarence J. Duffy, 2000, *Assessment of Uranium and Plutonium in the Saturated and Unsaturated Zones Beneath the Surface Disposal Area, INEEL*, LA-UR-00-5471, Los Alamos National Laboratory.

Roy, S. B. and D. A. Dzombak, 1997, "Chemical Factors Influencing Colloid-Facilitated Transport of Contaminants in Porous Media," *Environmental Science and Technology*, Vol. 31, No. 3, pp. 656–664.

Ryan, J. N. and M. Elimelech, 1996, "Colloid Mobilization and Transport in Groundwater," *Colloids and Surfaces A - Physicochemical and Engineering Aspects*, Vol. 107, pp. 1–56.

Ryan, J. N. and P. M. Gschwend, 1994, "Effects of Ionic-Strength and Flow-Rate on Colloid Release - Relating Kinetics to Intersurface Potential-Energy," *Journal of Colloid and Interface Science*, Vol. 164, No. 1, pp. 21–34.

Saiers, J. E. and J. J. Lenhart, 2003, "Colloid mobilization and transport within unsaturated porous media under transient-flow conditions," *Water Resources Research*, Vol. 39, No. 1, Article No. 1019.

Shaw, D. J., 1980, *Introduction to Colloid and Surface Chemistry*, ISBN: 0-40871049-7, Boston: Butterworth.

Stewart, K., 1963, "The Particulate Material Formed by the Oxidation of Plutonium," *Progress in Nuclear Energy Series IV*, Vol. 5, Oxford, England: Pergamon Press, pp. 535–579.

Thompson, J. L., 1989, "Actinide Behavior on Crushed Rock Columns," *Journal of Radioanalytical and Nuclear Chemistry-Articles*, Vol. 130, No. 2, pp. 353–364.

Wick, O. J., ed., 1984, *Plutonium Handbook*, Vols. I & II, ISBN: 0-89448-024-5, American Nuclear Society.

Yao, K. M., M. M. Habibian, and C. R. O'Melia, 1971, "Water and Waste Water Filtration - Concepts and Applications," *Environmental Science & Technology*, Vol. 5, No. 11, p. 1105.

Zodtner, L. L. and R. F. Rogers, 1964, *Study of Unaccounted-For Plutonium Losses*, U.S. Department of Energy.

Appendix A

Calculations and Parameters for Granular Filter Beds

Appendix A

Calculations and Parameters for Granular Filter Beds

The following equations used for calculations in Section 3.1.1 are derived from or summarized in Elimelech (1998). The meaning and unit value of terms used in the equations are listed in Table A-1. Two efficiency factors appear in the calculations. η_o expresses the fraction of colloids that are intercepted by collector grains and retained. This factor can be theoretically derived. The α expresses the fraction of theoretical attachment collisions that actually do result in colloid attachment. This factor is empirical and must be measured experimentally.

$L_T = -\ln\left(C_L / C_o\right)\left(\frac{4r_c}{3(1-f)\alpha\eta_o}\right)$, distance in porous media where colloid concentration is reduced from C_o to C_L

$\eta_o = 4A_s^{1/3}\left(\frac{D_\infty}{Ud_c}\right) + A_s N_{LO}^{1/8} R^{15/8} + 3.38\times10^{-3} A_s N_G^{1.2} R^{-0.4}$, collection efficiency based on the number of colloids that impact a collector grain impacting and retained by a collector

$D_\infty = kT / 6\pi r_p \mu$, spherical particle diffusion coefficient (Stokes-Einstein equation), (m^2/s)

$N_{LO} = 4H / 9\pi\mu d_p^2 U$, van der Waals number

$N_G = \left(\rho_p - \rho\right) g d_p^2 / 18\mu U$, gravitational force number

$A_S = 2\left(1-p^5\right) / \left(2-3p+3p^5-2p^6\right)$, porosity-dependent flow parameter

$p = (1-f)^{1/3}$

$R = d_p / d_c$, aspect ratio.

Table A-1. Meaning and unit value of terms used in Appendix A equations.

Symbol	Meaning	Units (value)
μ	Fluid viscosity	kg/(m s) (0.001)
ρ	Fluid density	kg/m^3 (1,000)
ρ_p	Colloid density	kg/m^3 (11,400 for PuO_2)
C_L	Colloid concentration at distance L	kg/m^3
Co	Initial particle concentration	kg/m^3
D_∞	Diffusion coefficient	m^2/s
d_c	Collector (sediment grain) diameter	m (see text)
r_c	Collector (sediment grain) radius	m (see text)
d_p	Colloid diameter	m (see text)
r_d	Colloid radius	m (see text)
f	Porosity	unitless
g	Gravitational constant	m/s^2 (9.8)
H	Hamaker constant	kg m^2/s^2 (1×10^{-20})
k	Boltzmann's constant	kg $m^2/(s^2$ K) (1.381×10^{-23})
T	Temperature	kelvin, K (see text)
U	Velocity	m/s (see text)